



Evaluation of the Various Aspects of the Progress in Clinical Applications of Laser Driven Ionizing Radiation

Katalin Hideghéty, Ákos Diósi, Máté Molnár, Róbert Polanek, Emilia Rita Szabó, Tünde Tőkés, Zoltán Szabó

3rd ELIMEDIC Workshop
CATANIA 2016.09. 7-9

SZÉCHENYI 

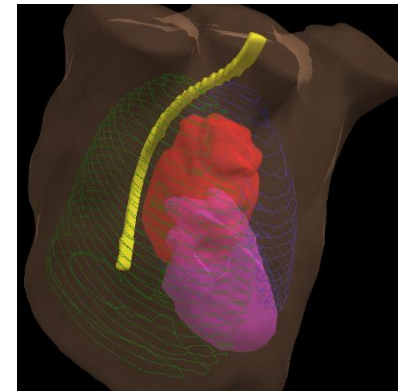
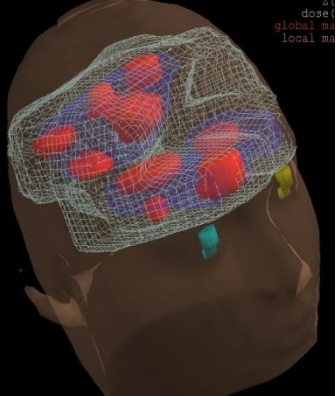


European Union
European Regional
Development Fund

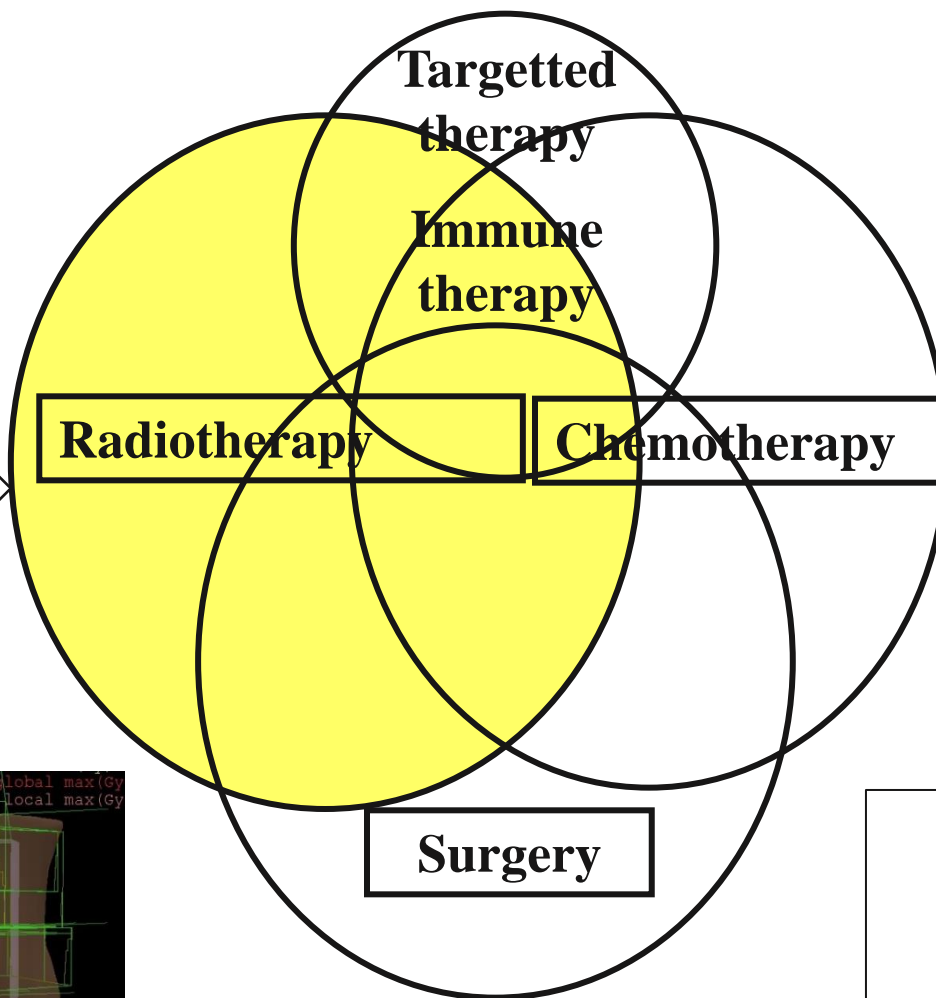


INVESTING IN YOUR FUTURE

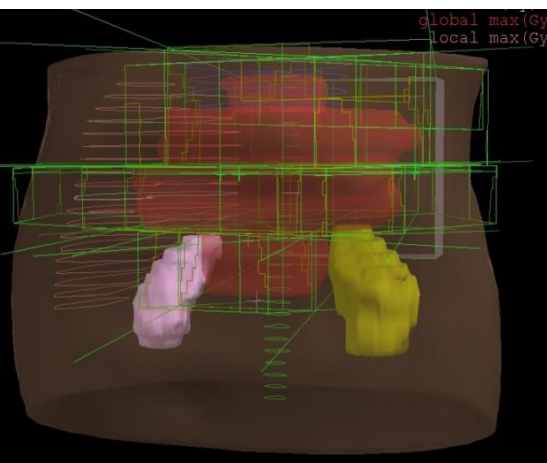
Complex tumor therapy



Advanced
diagnostics

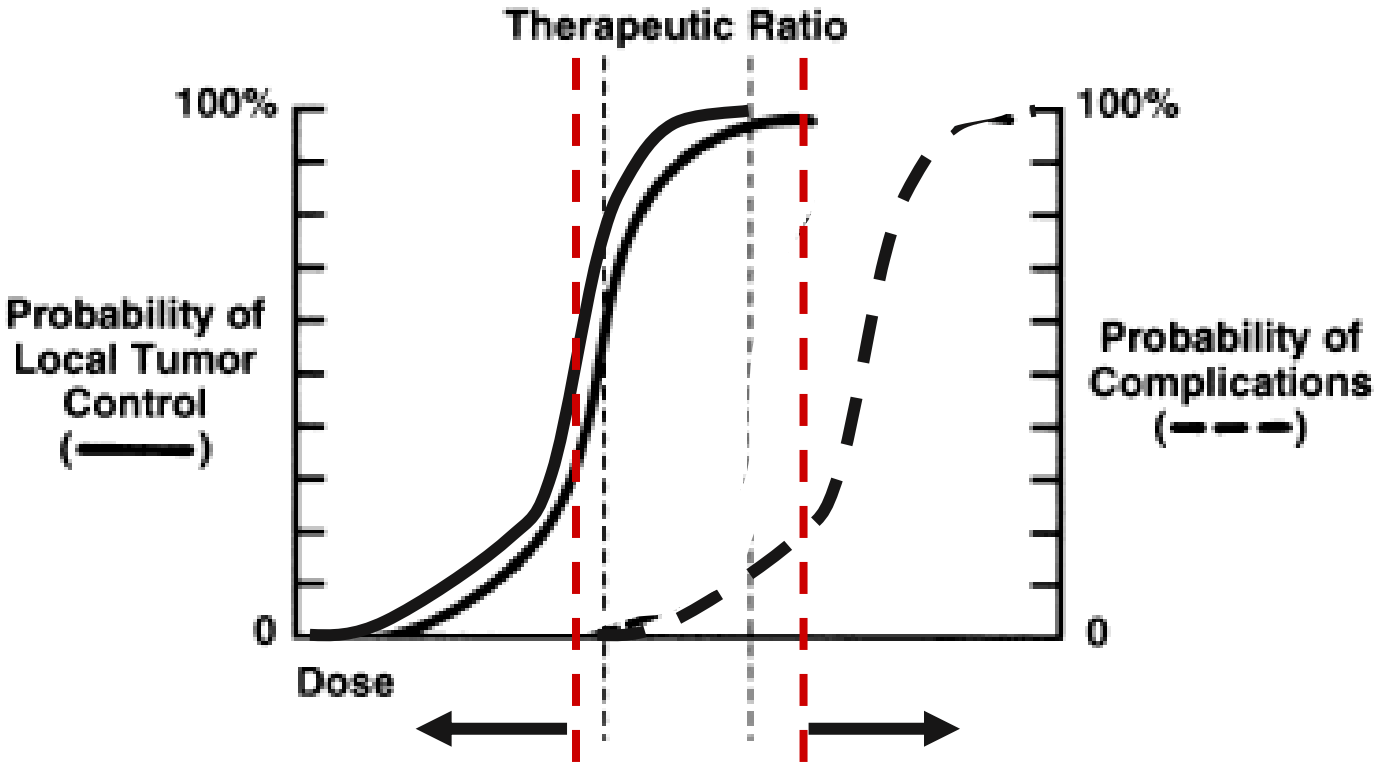


Improved
outcome



**10 million
patients/year
receive
radiotherapy**

Current approaches under **clinical** evaluation



Timing

Fractionation

Hypo-

Hyper-

Acceleration (CHART)

Prolongation

Combined treatment

sensitisation/protection

Chemo-, hormon, biol.m., hypoxic sens.

immunotherapy

Technical development

ConformalRT, IMRT, IGRT,
dose painting

Hadron therapy, BNCT

Diagnosis: Tu maxillo-cerebrale l.s. /first removal on 16.09.2015



Histology: Osteosarcom



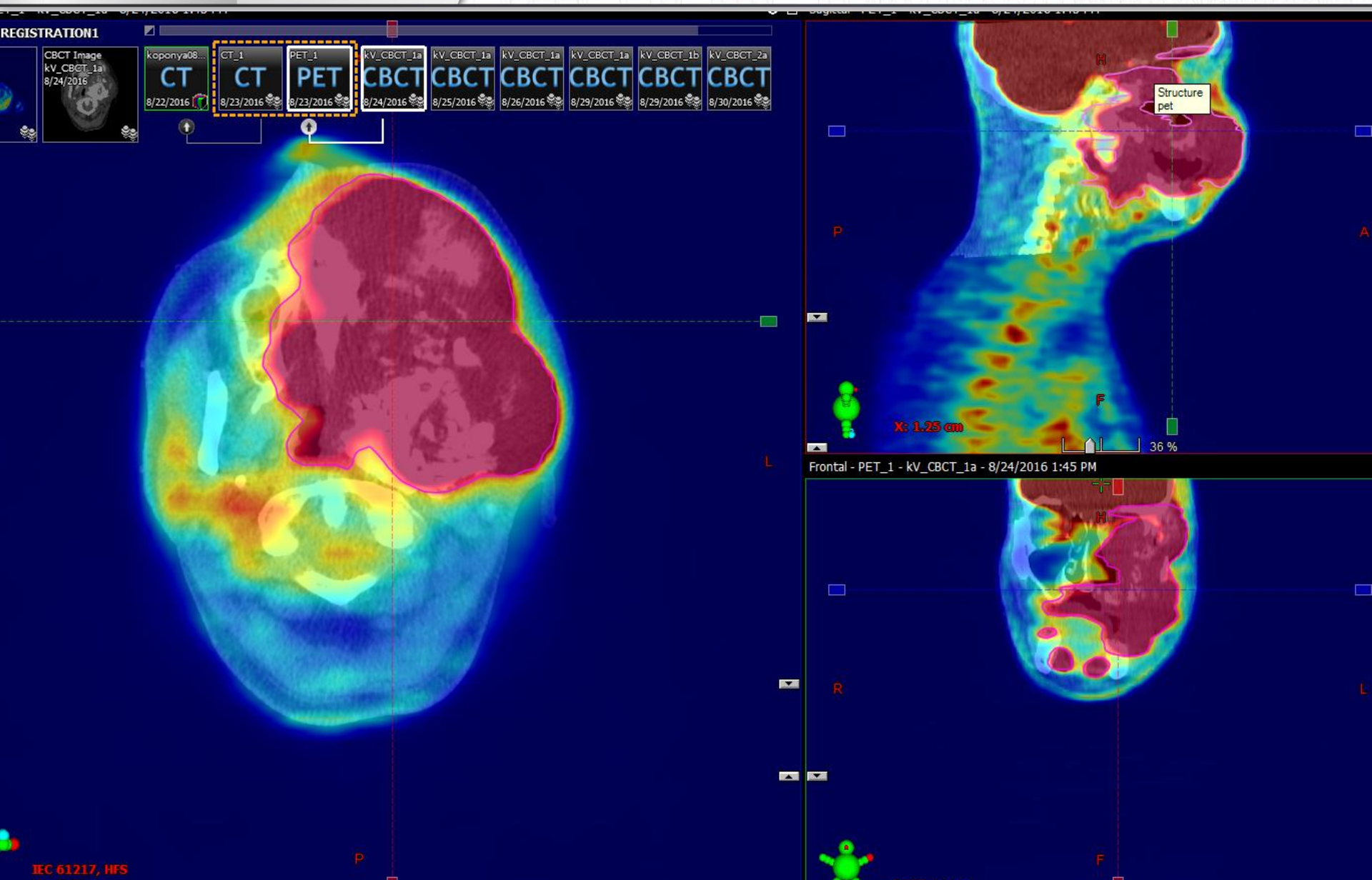
Adjuvant chemotherapy according to MAPIE protocol (6 cycles between 10.2015- 04.2016)

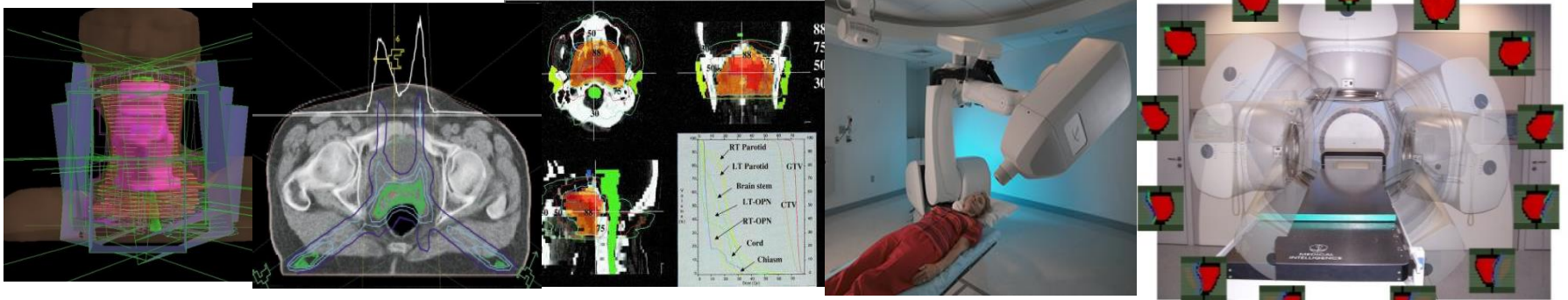
Reoperation because of progression (23.06.2016) R2

The second removal took place in common interdisciplinary (neurosurgeons-ENT experts) effort too. The majority of the high grade osteosarcom could be removed, but the postoperative MRI confirmed macroscopic residual tumor in critical location surrounded by radiosensitive structures.

Rapid clinical progression is detected

42 years old man with hypoxic inhomogeneous radioresistant tumor of the left maxilla





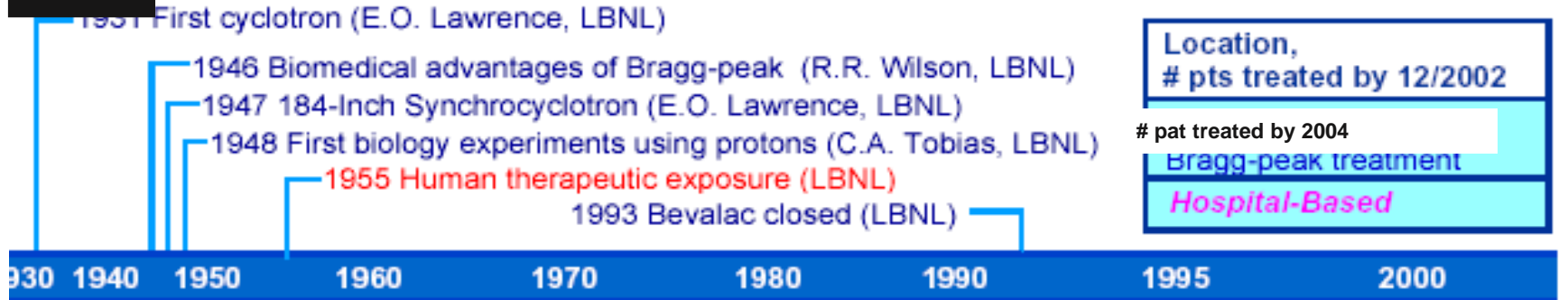
Photons 3-15 MeV, dose rate: 10 Gy/min

Selectivity, effectivity, accuracy

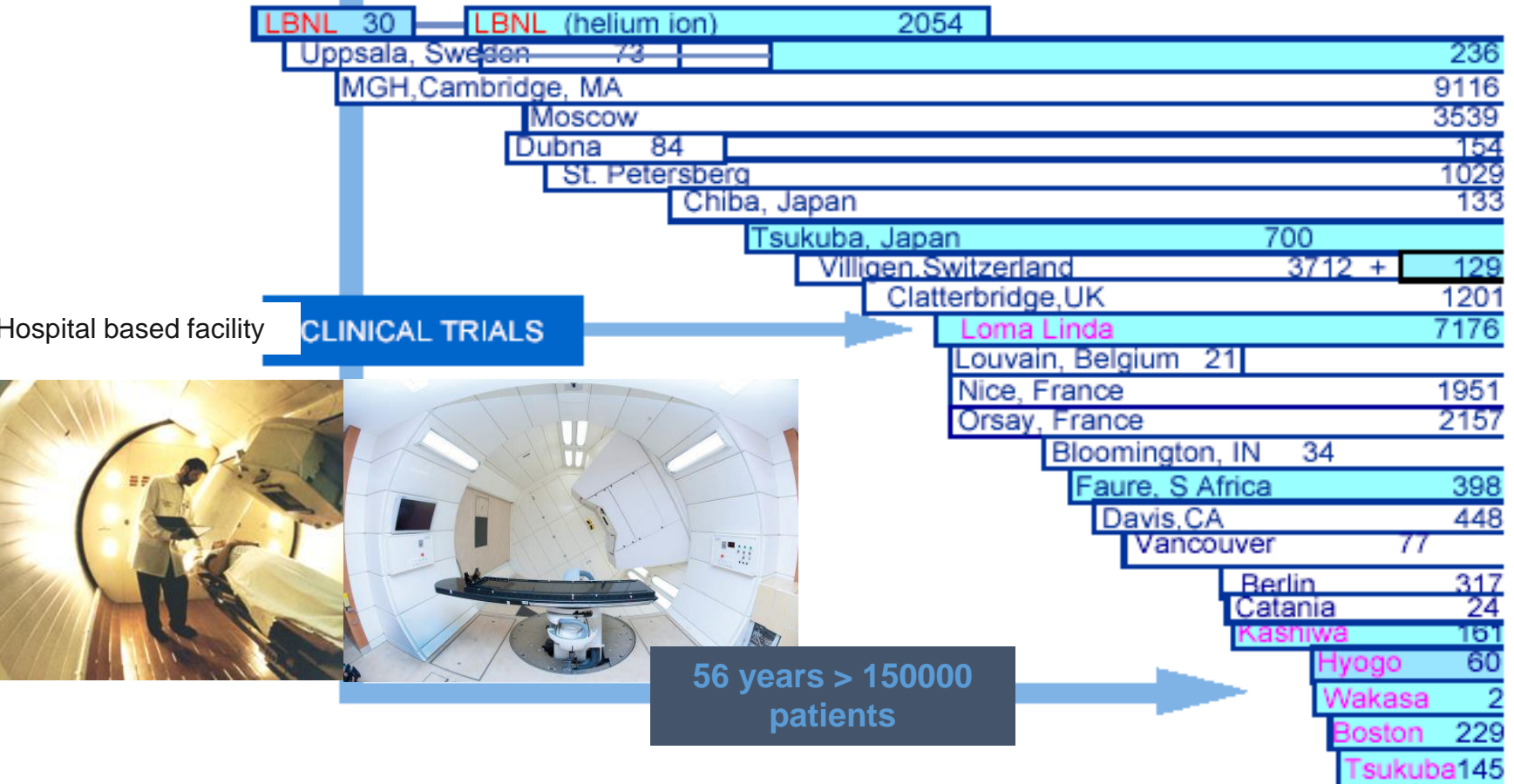
Hadron th.



Proton Therapy Scientific Milestones



Location, # pts treated by 12/2002
pat treated by 2004
Bragg-peak treatment
Hospital-Based



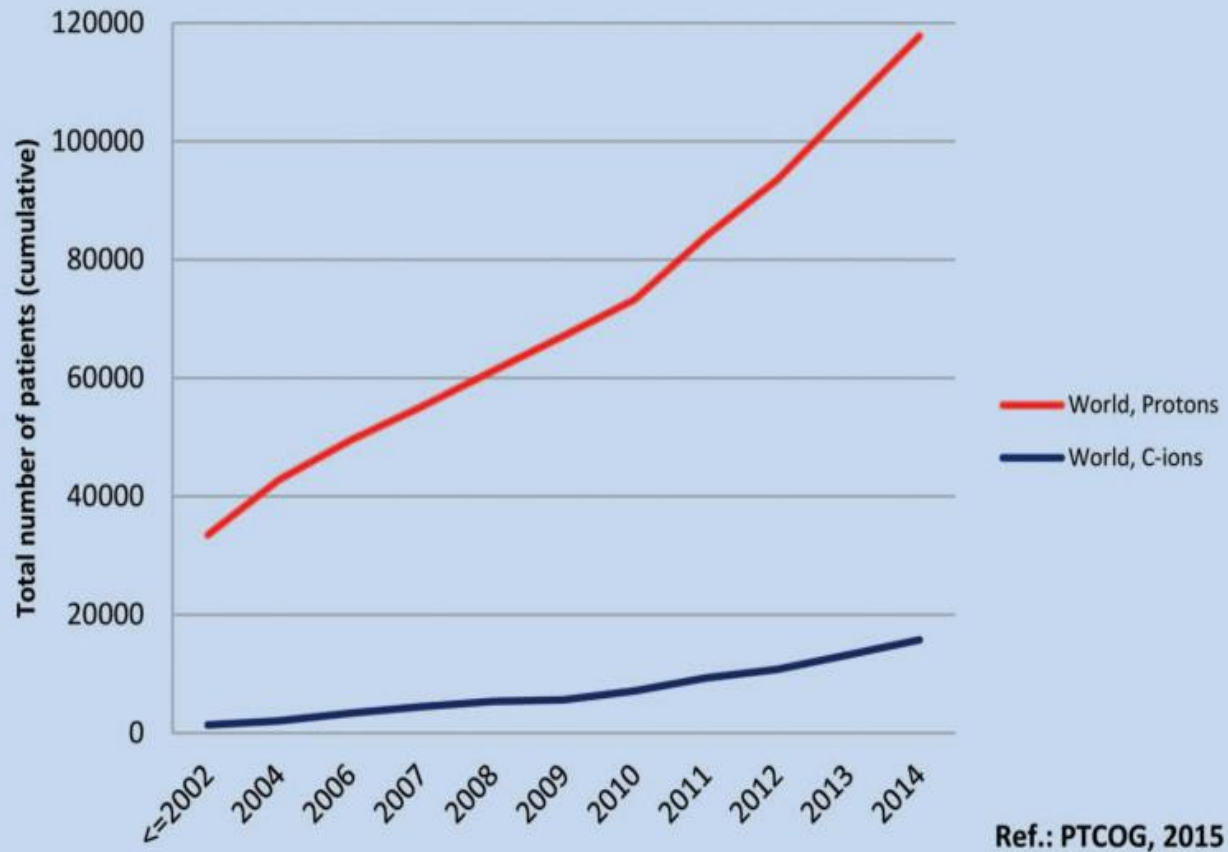
1st Hospital based facility

CLINICAL TRIALS



56 years > 150000 patients

Patients Treated with Protons and C-ions Worldwide

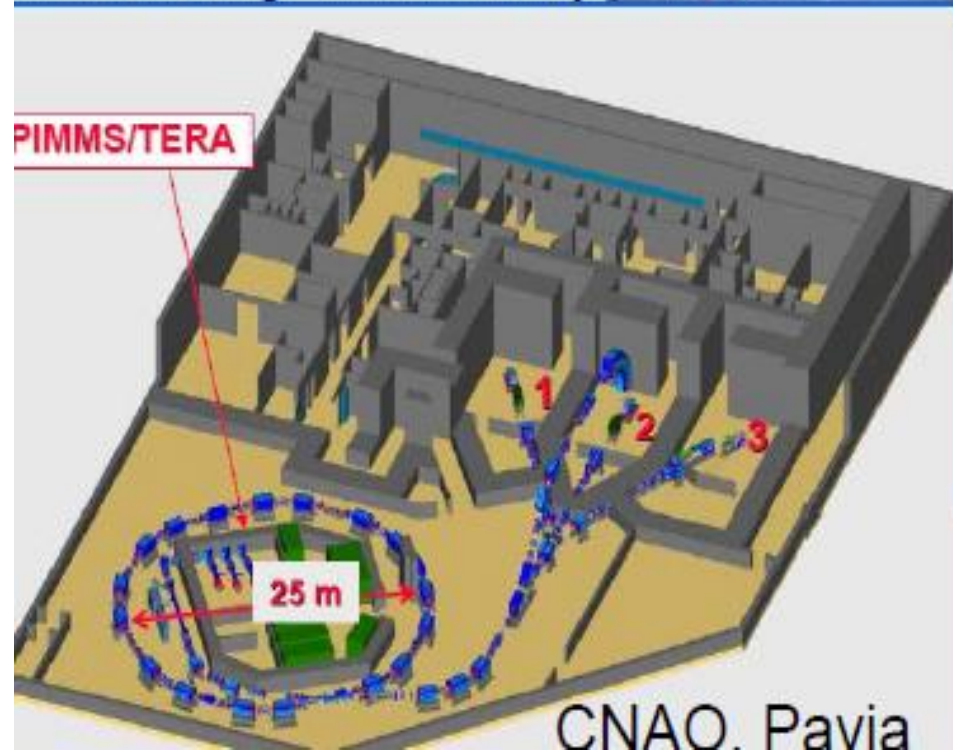
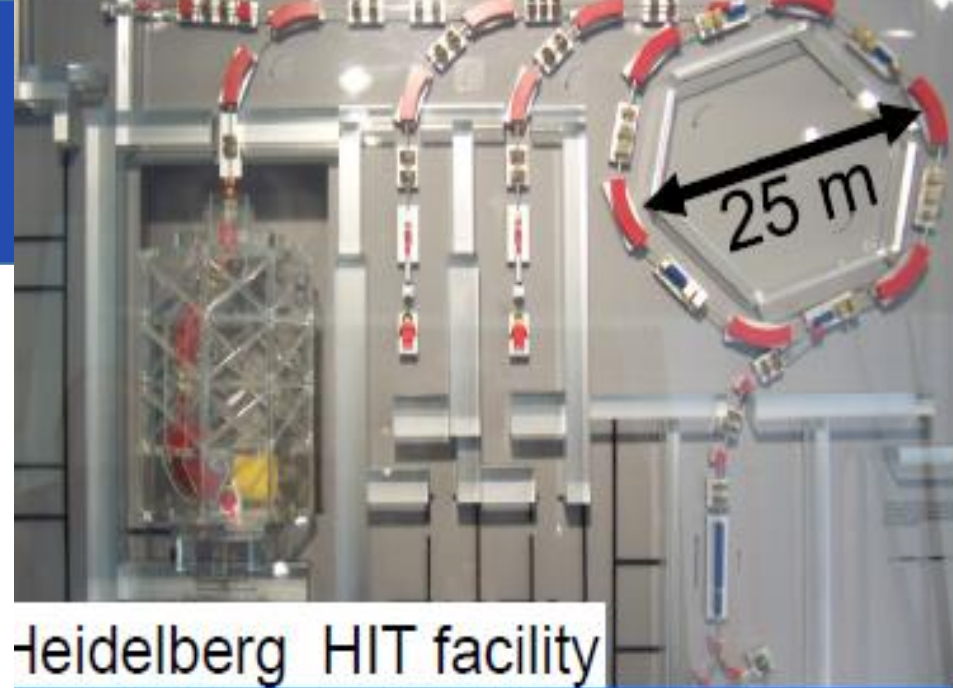


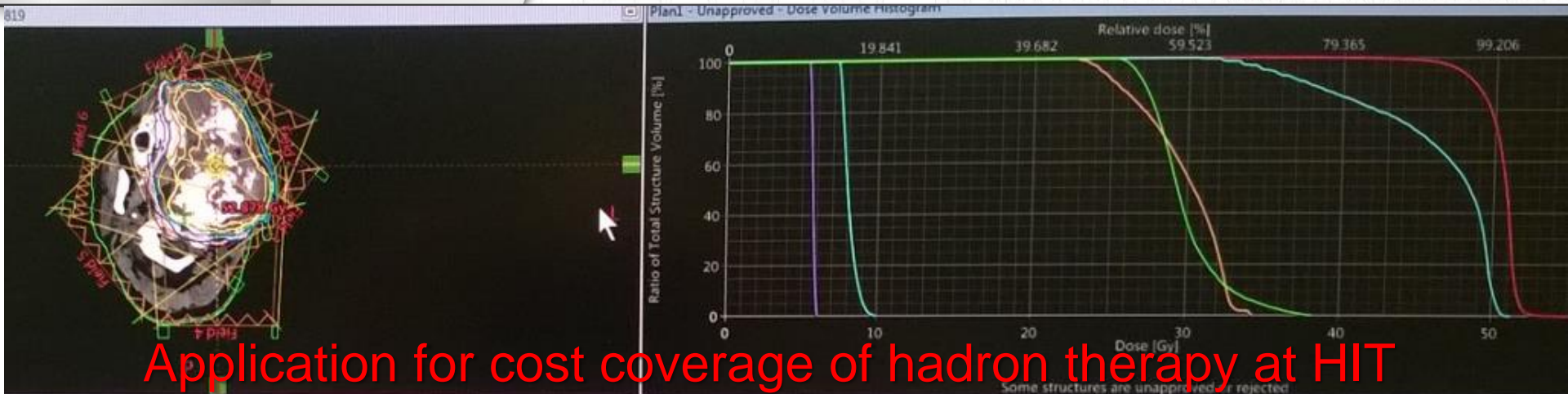
Total of all facilities (in and out of operation):

He	2054	1957-1992
Pions	1100	1974-1994
C-ions	15736	1994-present
Other ions	433	1975-1992
Protons	118195	1954-present
Grand Total	137179	

54 centers are in operation and further 40 is planned

<2% of all RT



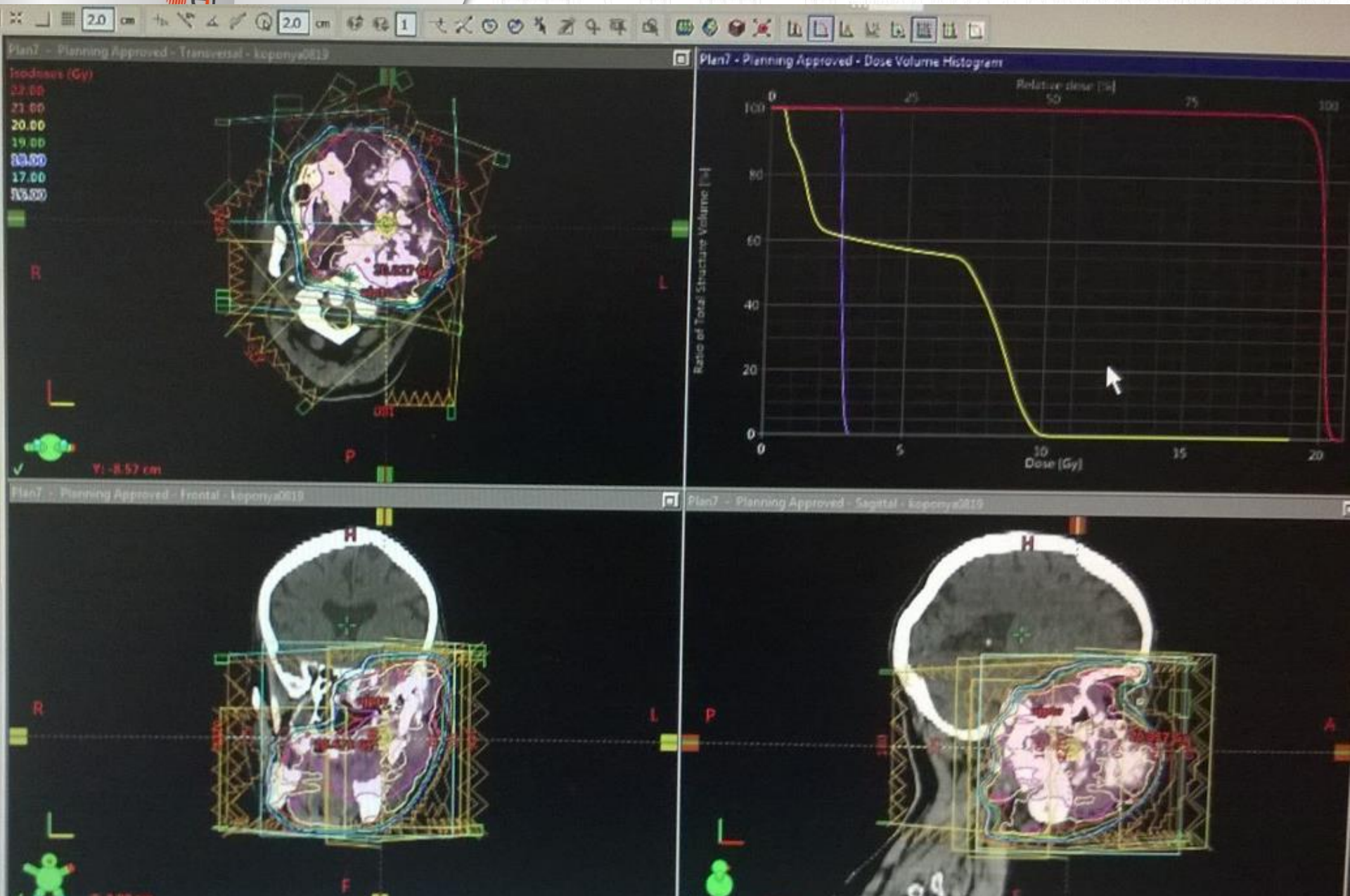


Application for cost coverage of hadron therapy at HIT

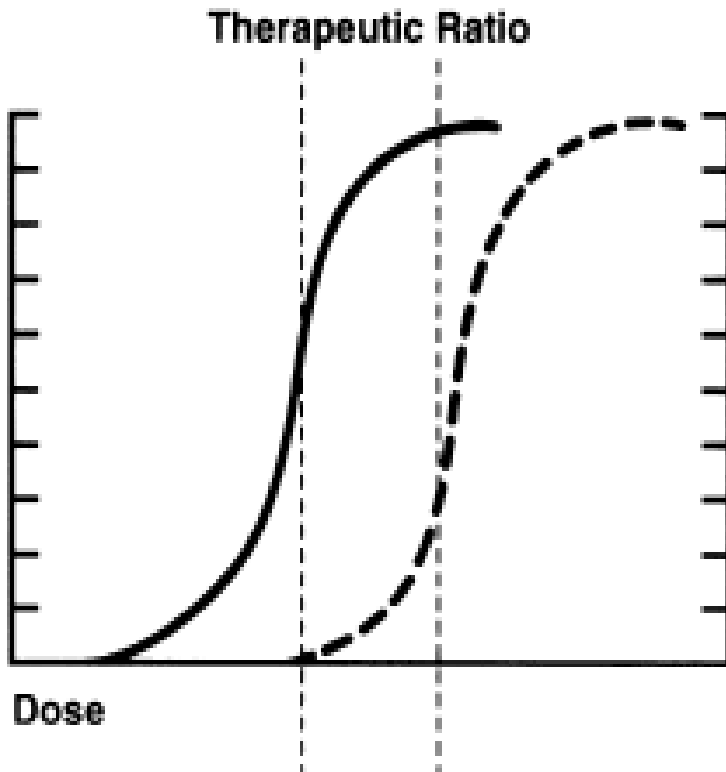


Course	Volume [cm ³]	Dose Cover. [%]	Sampling Cover. [%]	Min Dose [Gy]	Max Dose [Gy]	Mean Dose [Gy]
Cl		1.0	100.0			
Cl		0.9	100.0		25.138	38.436
Cl		0.4	100.0		30.503	51.306
Cl		0.2	100.0		22.110	34.399
Cl		0.2	98.6		7.241	10.073
Cl			99.4		5.316	6.144
Cl	751.7	100.0	100.0		34.753	55.309
Cl	6391.9	100.0	100.6		0.008	55.309

IMRT adaptive re-planing



Future approaches under **preclinical** evaluation



Increase of spatial resolution

- VHEE
- Mixed energy RT
- Mixed particle therapy
- Microbeam radiotherapy
- Dose and LET painting

Timing

Pulsed radiation

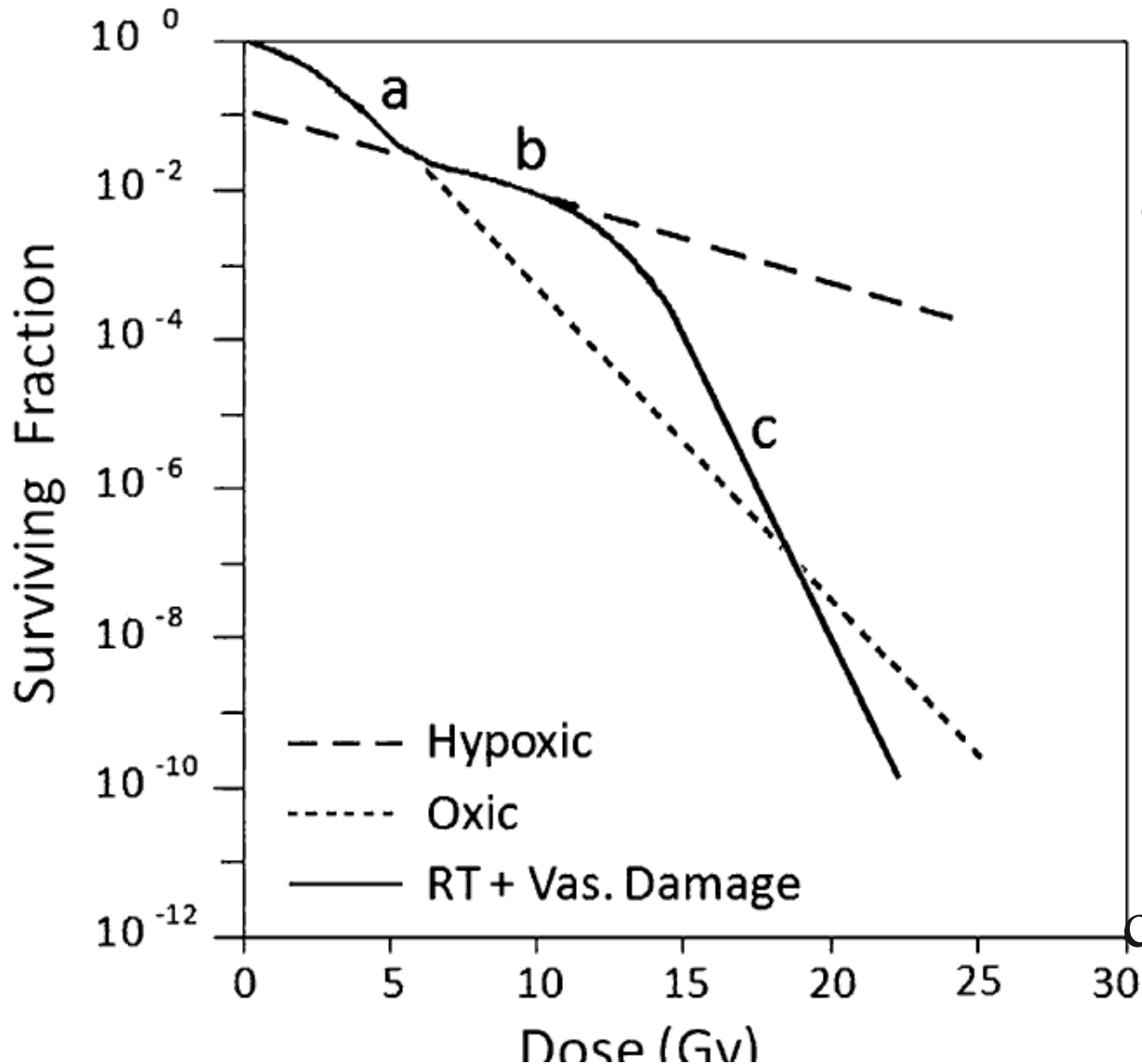
Flash irradiation

Combined treatment

Novel chemo-, hormon, molecular approaches (DBAIT) immunotherapy

Neutron capture/boron proton fusion

Large fraction dose – short time



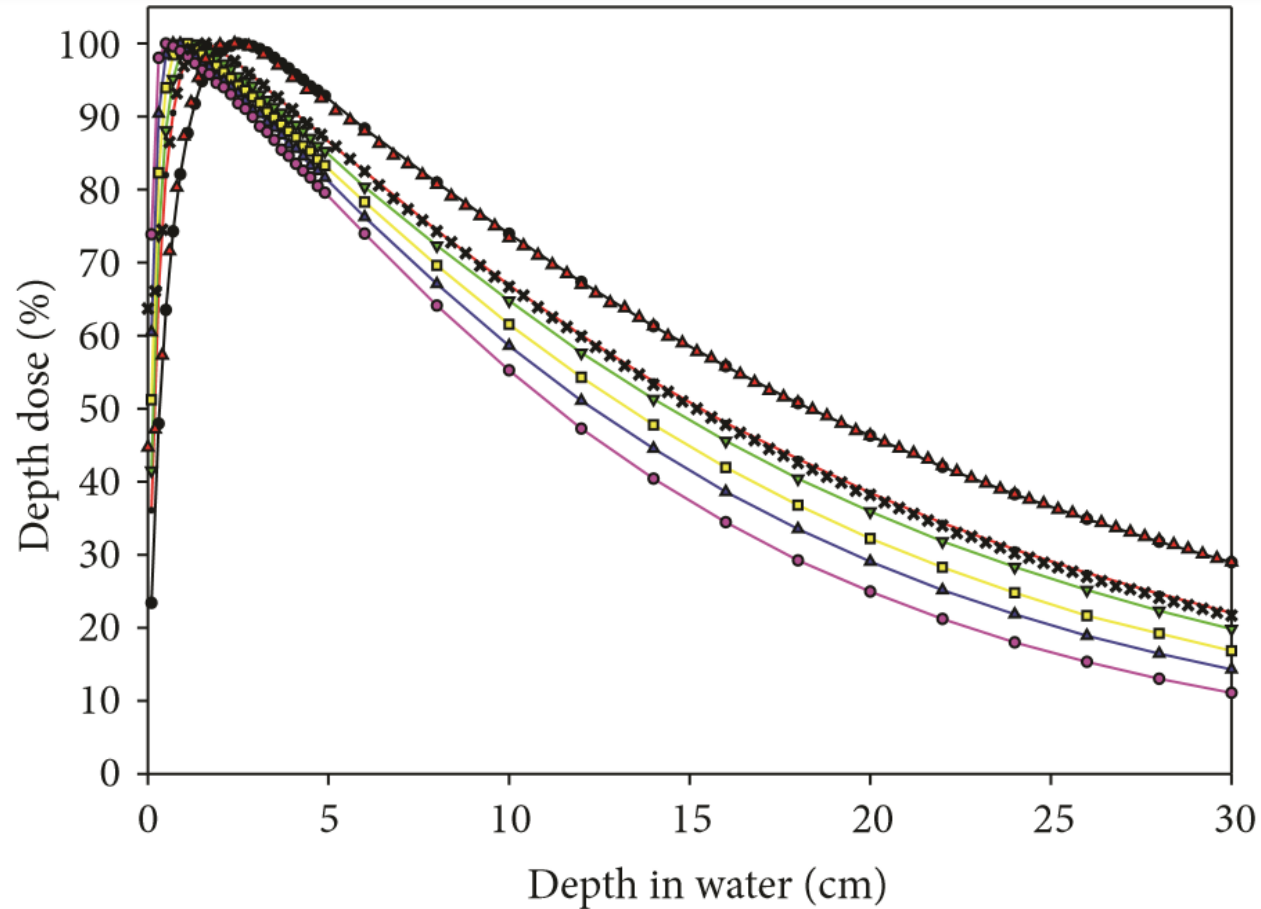
The functional vascularity in tumors decreases within several hours after irradiation with doses higher than 10–15 Gy.



Decrease of tumor stem cells, because tumor perivascular niche is the home of cancer stem cells state

Energy Modulated Photon Radiotherapy: A Monte Carlo Feasibility Study

Y. Zhang, Y. Feng, XinMing, and J. Deng



- Monte Carlo 10 MV
- Monte Carlo 6 MV
- ▼— Monte Carlo 5 MV
- Monte Carlo 4 MV

- ▲— Monte Carlo 3 MV
- Monte Carlo 2 MV
- * Measurements 6 MV
- ▲ Measurements 10 MV

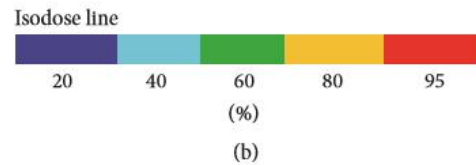
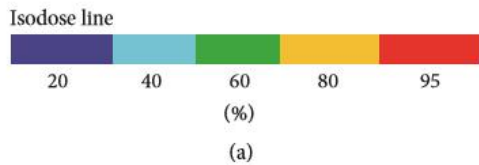
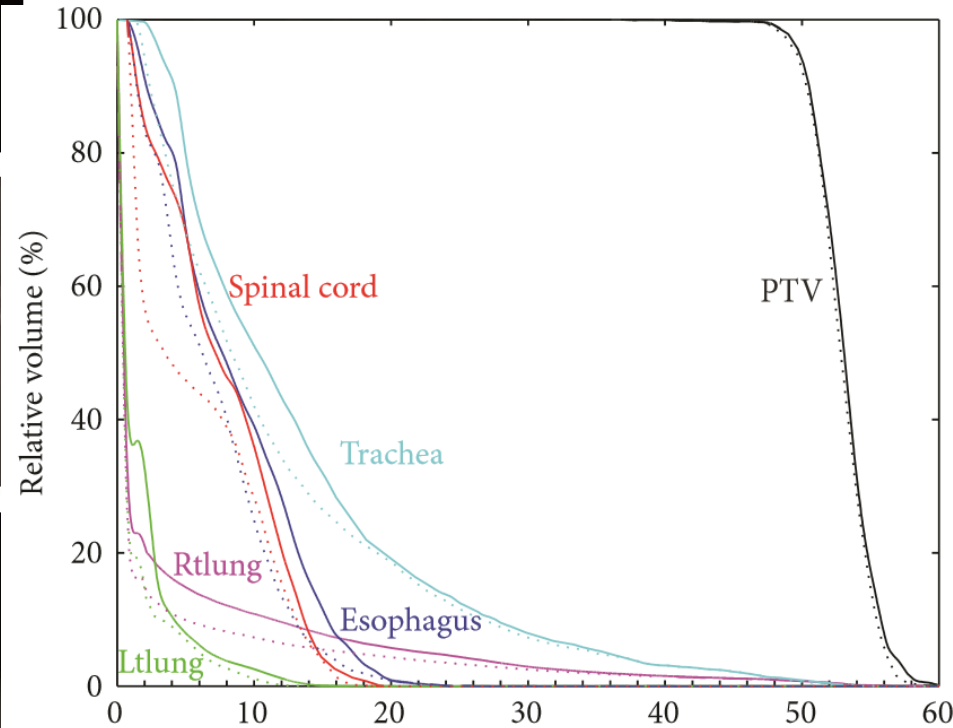
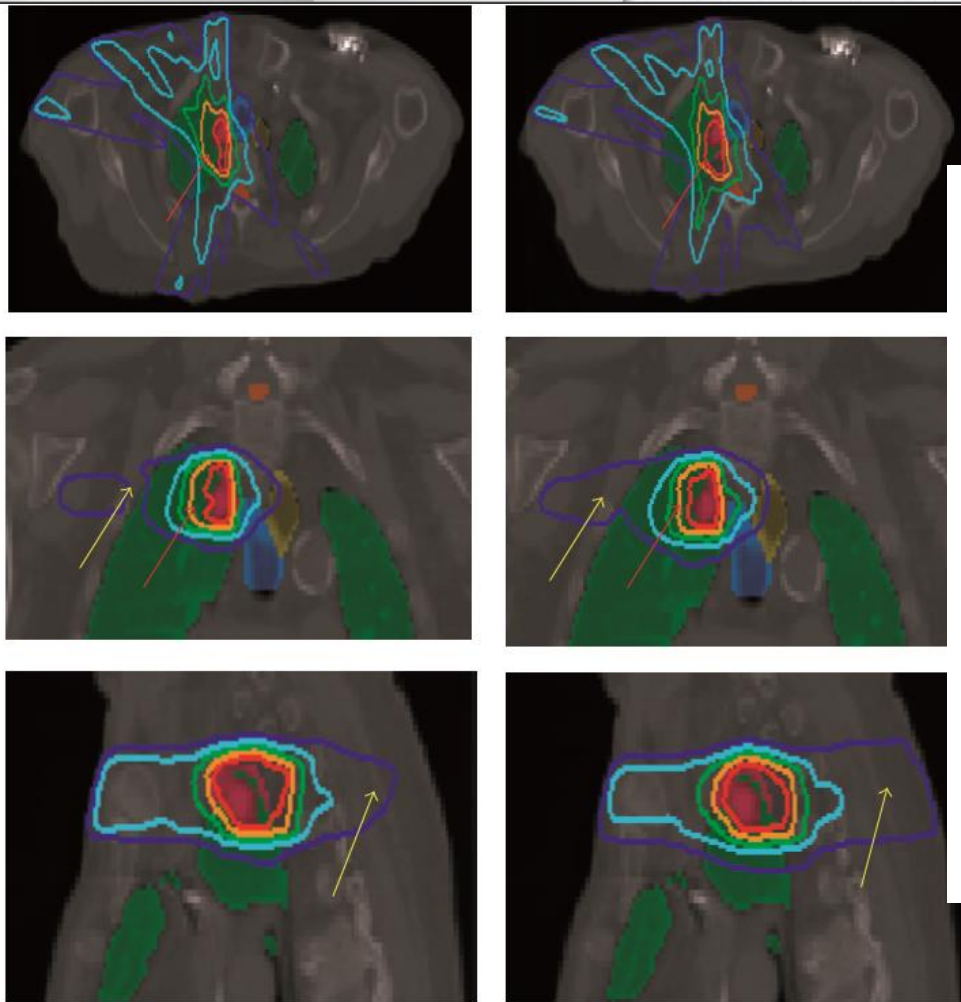


Comparison of EMXRT dose distribution to IMRT

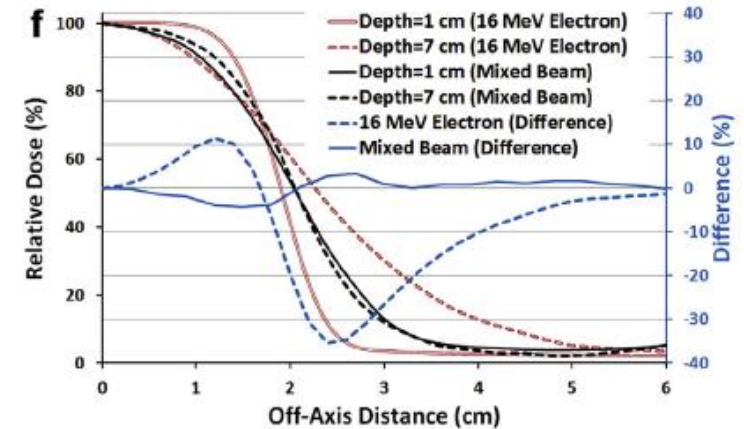
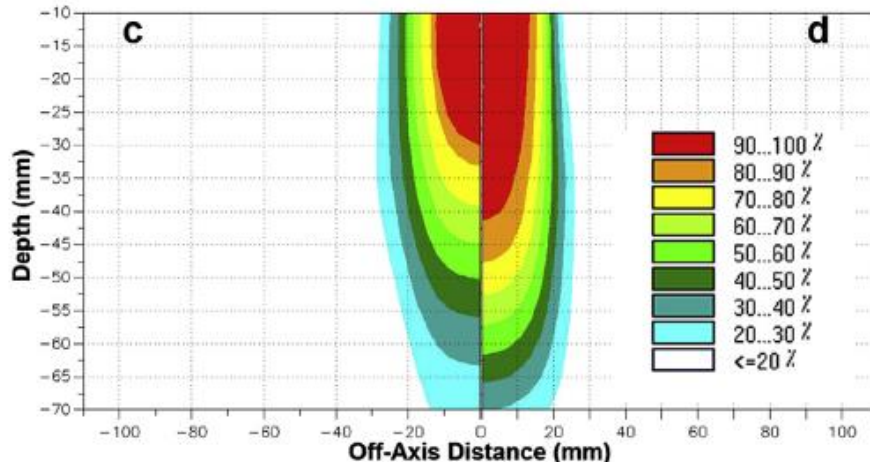
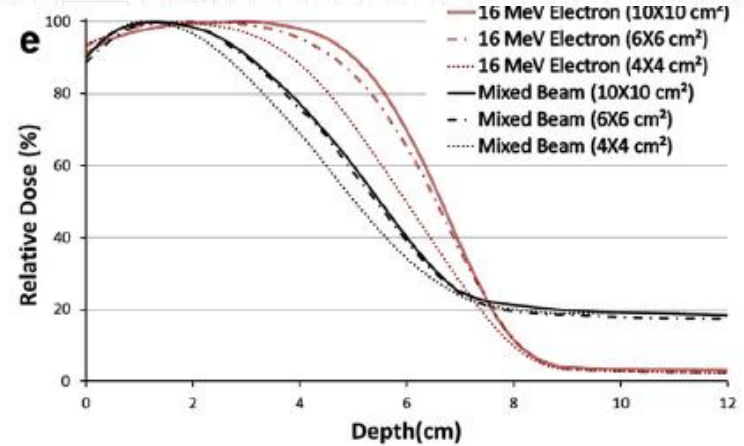
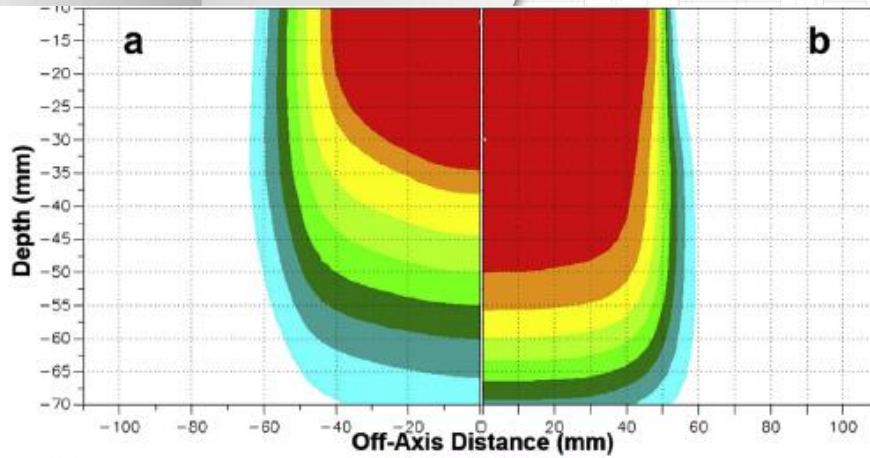
Tumor site	OARs	Indices	IMRT/Gy	EMXRT/Gy	Relative difference* /%
Prostate	Rectum	D_{mean}	32.5	31.5	-3.1
		$D_{15\%}$	49.7	50.7	+2.1
	Bladder	D_{mean}	34.0	33.8	-0.6
		$D_{15\%}$	57.9	57.3	-1.0
	Femur head	D_{mean}	10.6	13.7	+29.2
		$D_{15\%}$	15.4	21.9	+42.2
Head and neck	Spinal cord	D_{mean}	14.3	13.9	-2.8
		D_{max}	44.7	45.2	+1.1
	Brainstem	D_{mean}	14.0	13.5	-3.6
		D_{max}	44.6	43.1	-3.4
	Mandible	D_{mean}	31.2	31.6	+1.3
		D_{max}	82.1	80.3	-2.2
	Left parotid	D_{mean}	13.4	14.9	+11.2
	Right parotid	D_{mean}	26.7	28.6	+7.1
Lung	Spinal cord	D_{mean}	7.7	6.3	-18.2
		D_{max}	19.4	17.2	-11.3
	Left lung	D_{mean}	3.5	2.6	-25.7
	Right lung	D_{mean}	1.7	1.1	-35.3
	Trachea	D_{mean}	13.1	12.9	-1.5
	Esophagus	D_{mean}	8.5	7.4	-12.9
Spine	Spinal cord	D_{mean}	4.9	4.7	-4.1
		D_{max}	15.9	14.6	-8.2
	Liver	D_{mean}	1.3	1.2	-7.7
	Kidneys	D_{mean}	0.3	0.3	0.0
Brain	Brainstem	D_{mean}	6.3	5.9	-6.3
		D_{max}	20.2	20.2	0.0
	Eyes	D_{max}	3.1	2.7	-12.9
	Chiasm	D_{max}	2.6	2.4	-7.7
Thyroid	Spinal cord	D_{mean}	17.6	16.0	-9.0
		D_{max}	41.6	40.6	-2.3
	Esophagus	D_{mean}	44	43.3	-1.7
	Trachea	D_{mean}	43.2	42.0	-2.7
	Pharynx	D_{mean}	8	9.7	+21.1

*Relative difference = $100\% \times (\text{Index}_{\text{EMXRT}} - \text{Index}_{\text{IMRT}}) / \text{Index}_{\text{IMRT}}$. The "+" and "-" indicate whether the dose index of the EMXRT plan is larger or smaller than that of IMRT plan. D_{mean} is the mean dose, and D_{max} is the maximum dose.

Comparison of EMXRT dose distribution to IMRT for lung tumor irradiation



N. Khaledi et al. Simultaneous production of mixed electron-photon beam in a medical LINAC: A feasibility study *Physica Medica* 31 (2015) 391-397



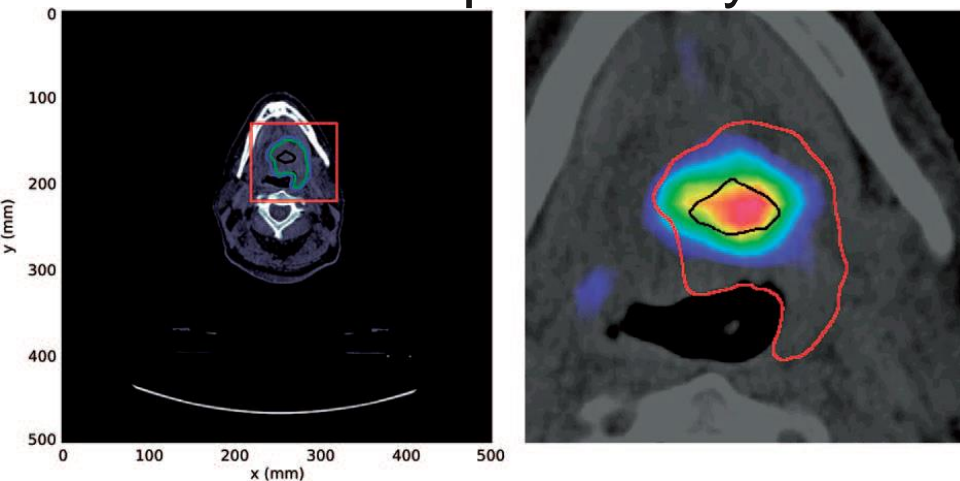
The advantages of mixing the electron and photon beam is reduction of pure electron's penumbra dependency with the depth, especially for small fields, also decreasing of dramatic changes of PDD curve with irradiation field size.

Dose- and LET-painting with particle therapy. Bassler

N, Jäkel O, et al. *Acta Oncol.* 2010 Oct;49(7):1170-6.



Simultaneous dose and LET optimisation has a potential to achieve higher tumour control and/or reduced normal tissue control probability.



LET-painting increases tumour control probability in hypoxic tumours

N. BASSLER J.TOFTEGAARD et al.
Acta Oncologica

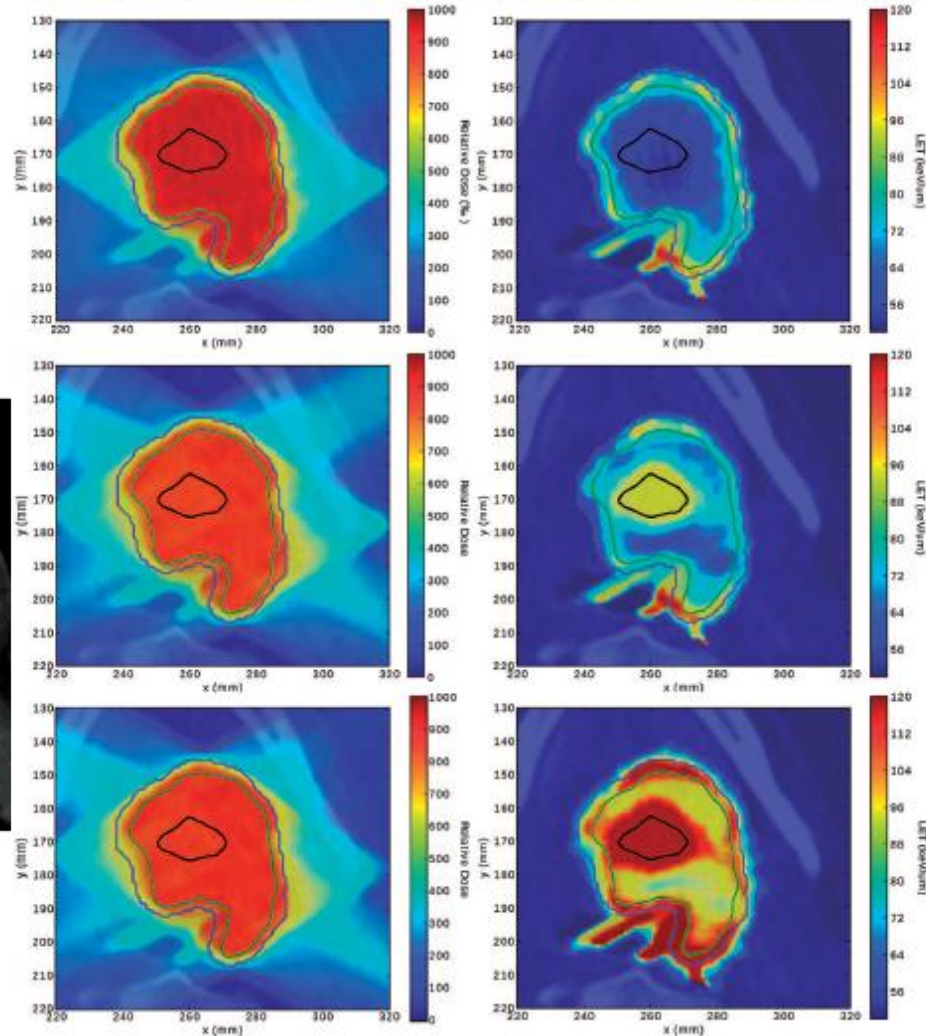


Figure 3. Dose and dose-averaged LET profiles shown in left and right column, respectively. First row is a carbon-12 ion plan using four conventional fields with homogeneous dose. The highest LET is then found at the rim of the SOBPs as seen in the upper right figure. LET-painting, as shown in the middle row, allows for redistributing LET to cover the assumed hypoxic structure, depicted as the black entity, with increased LET. The energy fluence budget for the amount of particles used is the same for both plans in the upper two rows. The last row shows LET-painting again, but now with oxygen-16 ions, resulting in a pronounced increase of LET in the HTV. HTV, hypoxic target volume; LET, linear energy transfer; SOBPs, spread out Bragg peak.

Proton/ion acceleration techniques

cyclotron

synchrotron

Small
synchro-
cyclotron

cyclotron
driven linac

Dielectr. wall
linacs

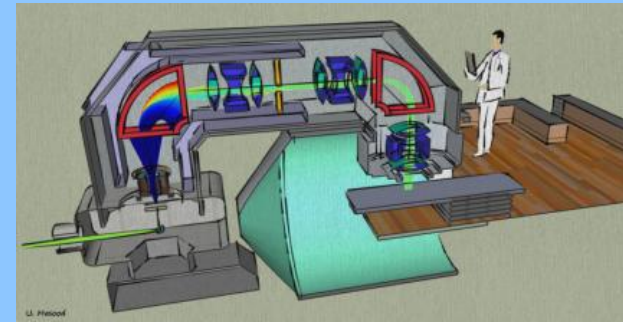
FFAG

Fixed Field Alternating
Gradient

lasers

Plasma
wake field

Compact EIMCPT design



<http://phys.org/news/2014-06-compact-proton-therapy-cancer.html>



Boron Neutron Capture Therapy (BNCT) for GBM at the Petten facility- European phase I study

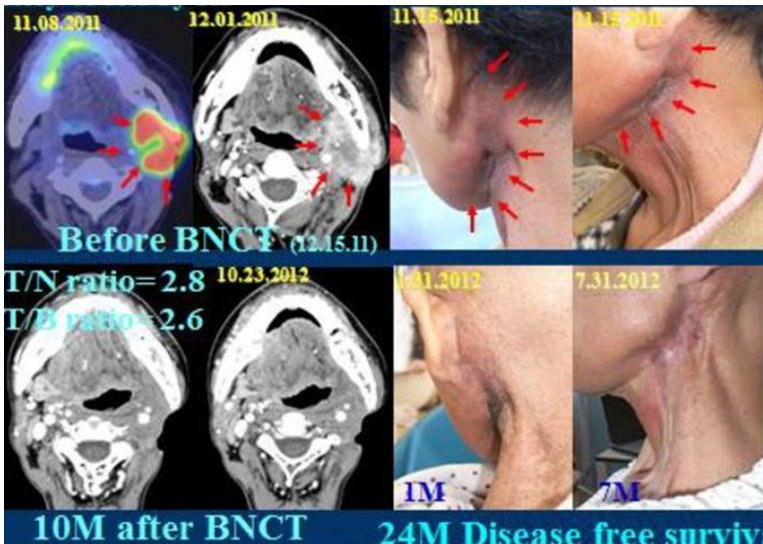


HFR Research reactor

Boron carrier

BSH

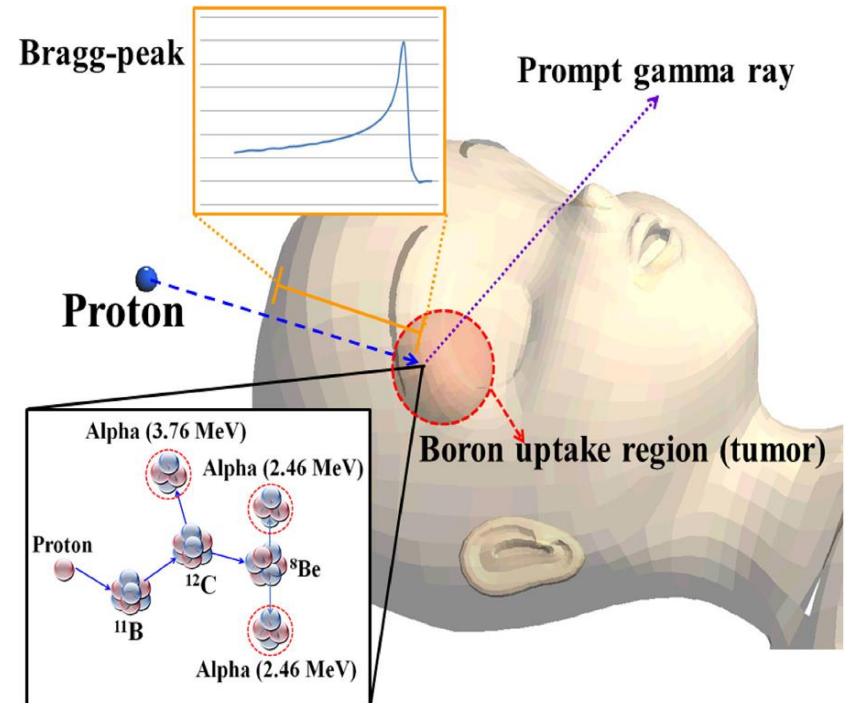
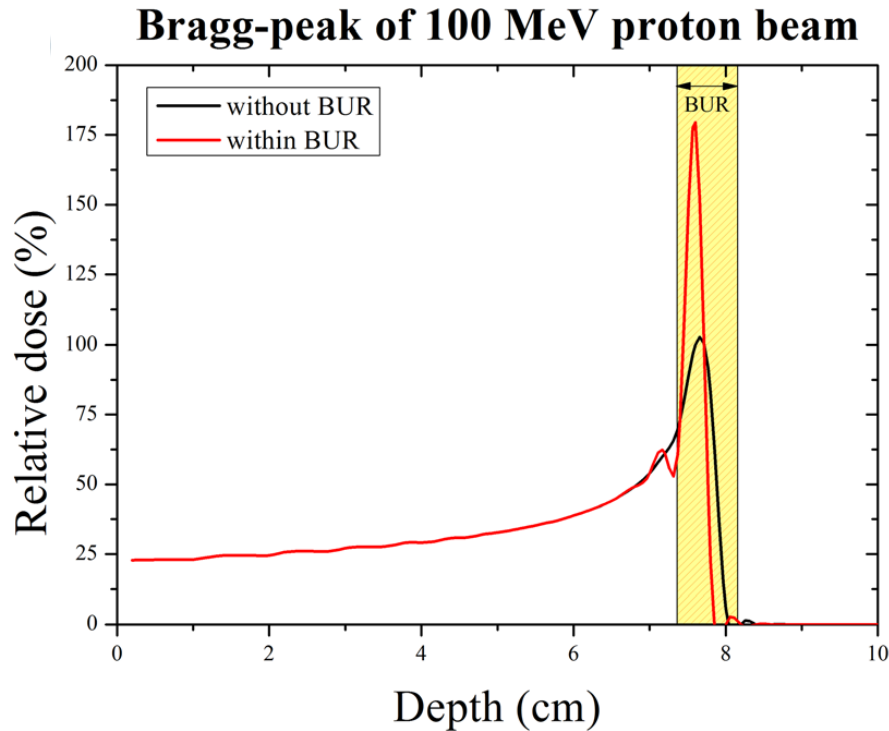
$\text{Na}_2\text{B}_{12}\text{H}_{11}\text{SH}$



Recurrent
H&N tumors

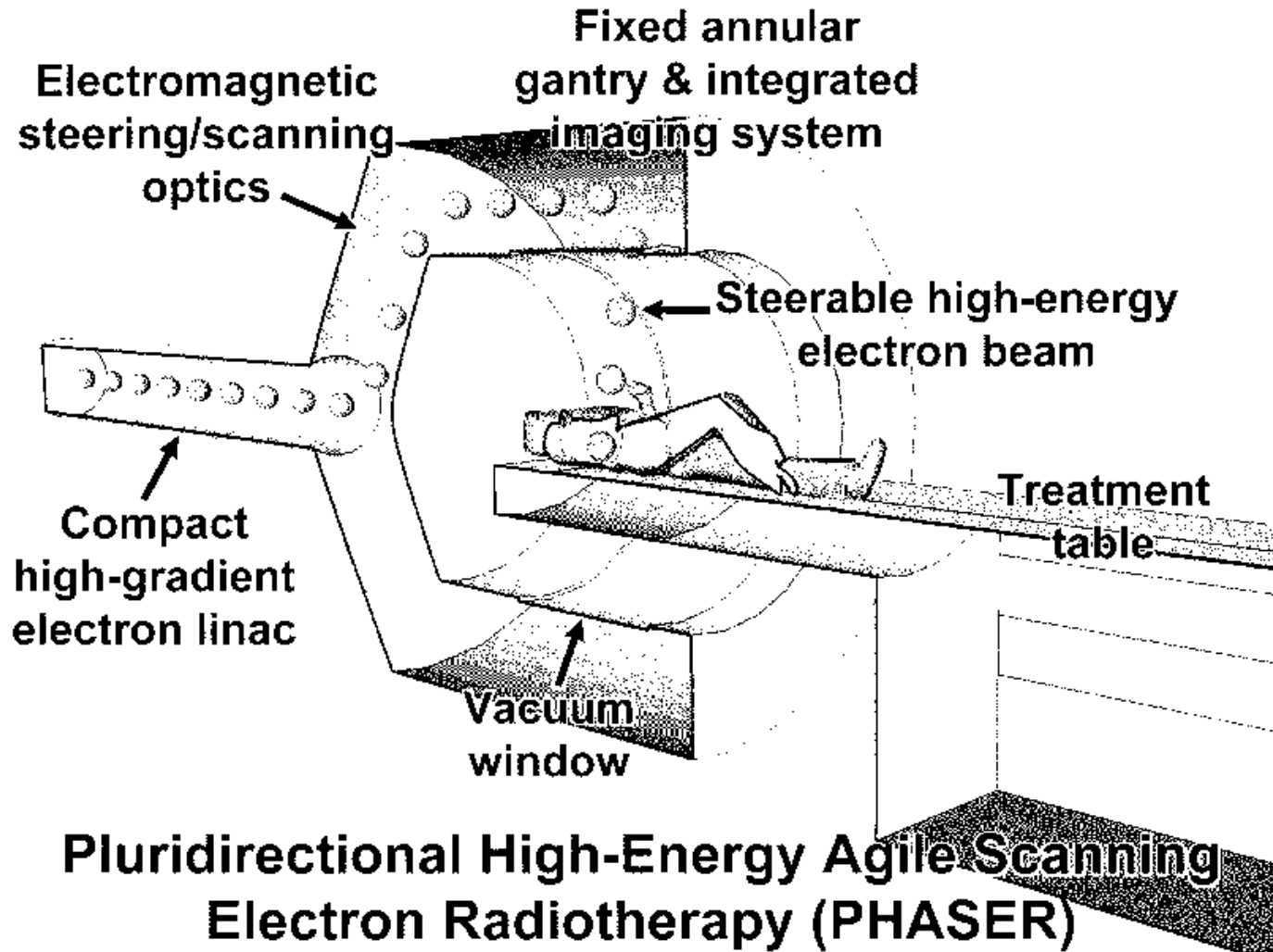
Boron carrier
BPA

Yoon DK, Jung JY, Suh TS. **Application of proton boron fusion reaction to radiation therapy: a Monte Carlo simulation study.** Appl Phys Lett. 2014;105:223507.



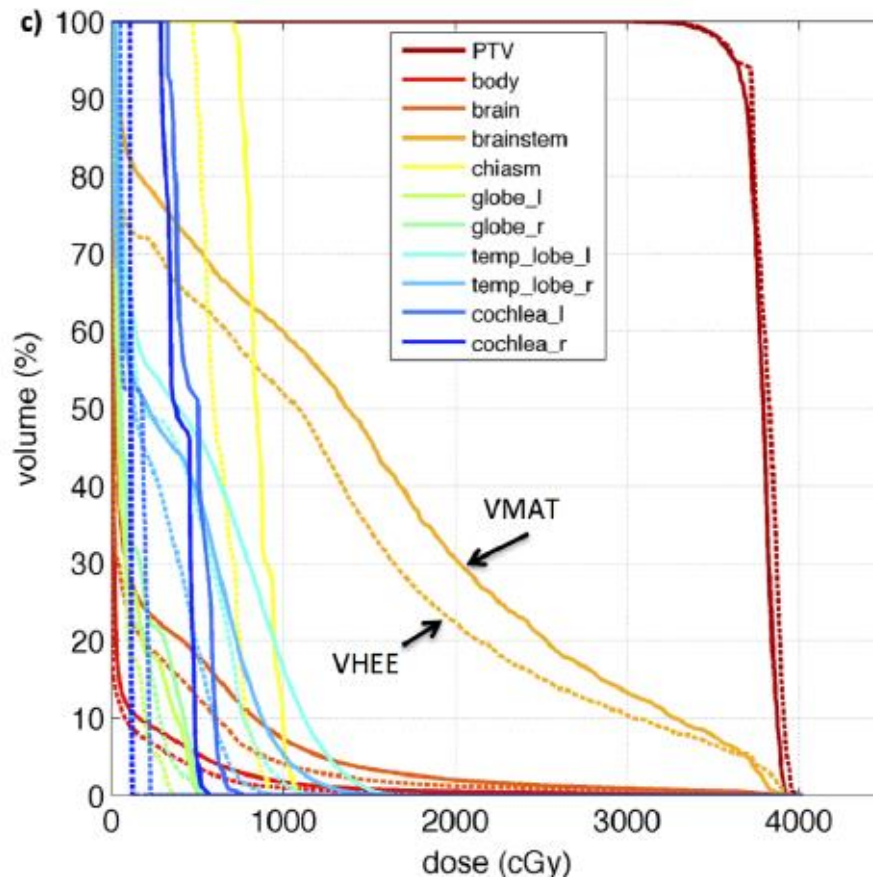
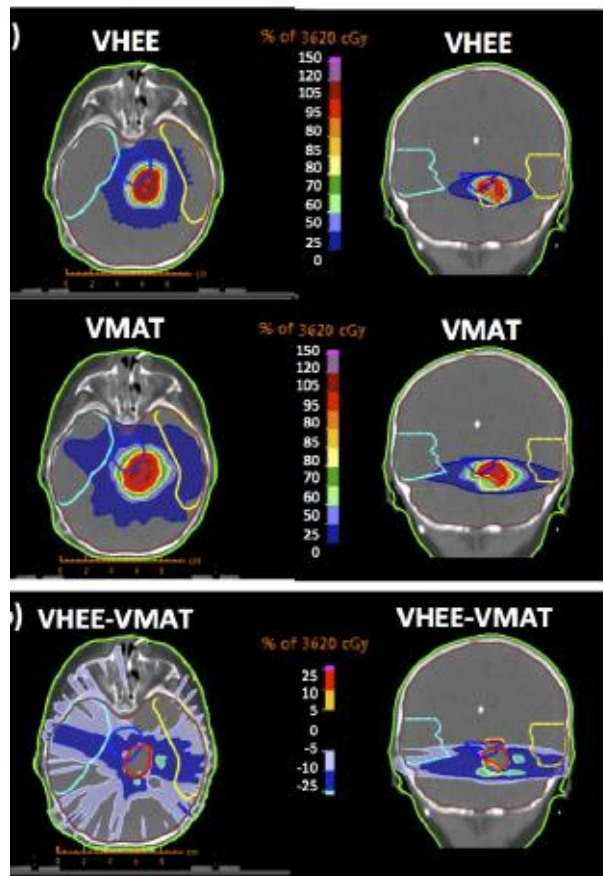
After the proton reacts with the boron (^{11}B), the boron changes to carbon (^{12}C) in an excited state. The excited carbon nucleus is split into alpha particle of 3.76 MeV and beryllium (^8Be). Subsequently, the beryllium is divided into the two alpha particles of 2.74 MeV each. The maximum point of the Bragg-peak is increased by the boron at the BUR. In addition, the prompt gamma ray emitted by the reaction can provide information about the therapy region.

Multifield Very High Energy Electron accelerator



**Pluridirectional High-Energy Agile Scanning
Electron Radiotherapy (PHASER)**

The dosimetric advantage of VHEE radiotherapy over photon VMAT radiotherapy was demonstrated for different clinical cases (pediatric, lung, liver, esophage, prostate).



VHEE dose to all critical organs was up to 70% lower than the clinical 6 MV VMAT dose for the same target and the integral dose was decreased by 33% compared to the VMAT plan.

Palma B, et al Assessment of the quality of very high-energy electron radiotherapy planning Radiother Oncol. 2016 Apr;119(1):154-8.

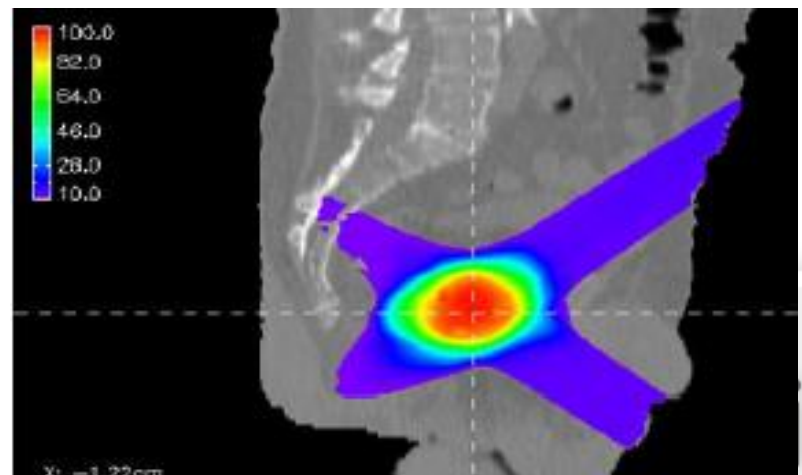
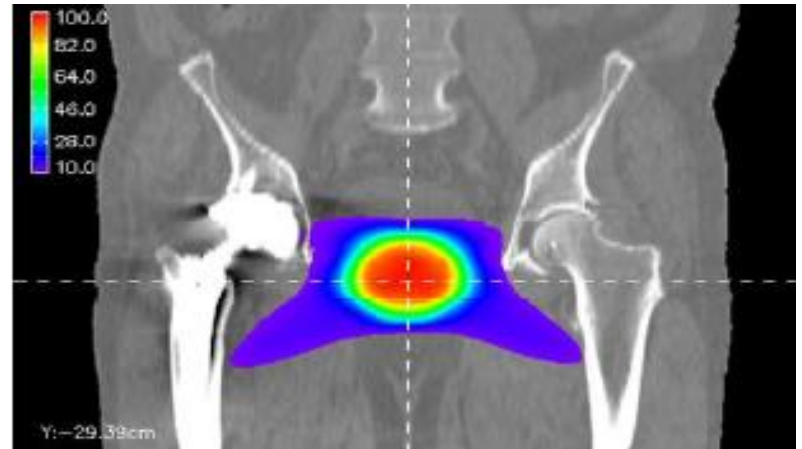
Bazalova-Carter M. et al. Treatment planning for radiotherapy with very high-energy electron beams and comparison of VHEE and VMAT plan. Med Phys. 2015 May; 42 (5): 2615-2

C, DesRosiers, V. Moskvina, M. Caoa, C. J. Joshib, M. Langera **Laser-plasma generated very high energy electrons in radiation therapy of the prostate**

Monte Carlo simulation of radiation treatment by laser accelerated very high energy (200 MeV) electron VHEE.

Small diameter VHEE beamlets can be scanned, thereby producing a finer resolution intensity modulated treatment than photon beams.

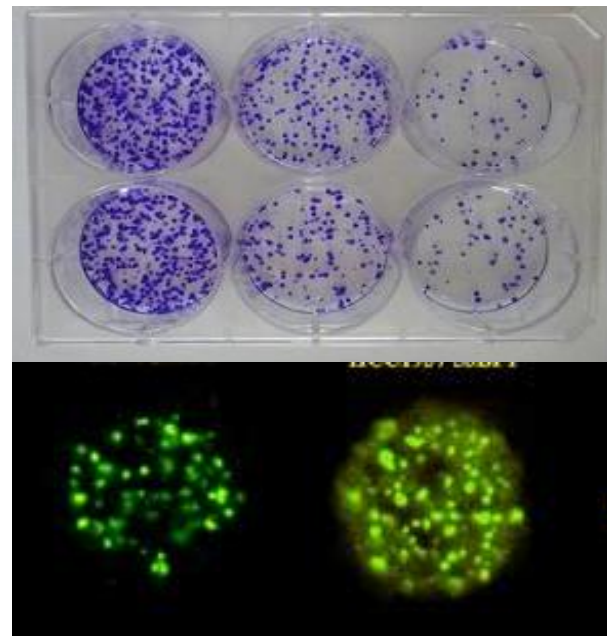
A VHEE accelerator may be optimally designed using laser-plasma technology



Results on radiobiology experiments on laser driven ionizing RT sources



Up to now the results of both in vitro, and in vivo experimental data reveal no evidence for a substantially different radiobiology effect of **laser accelerated particles (electron/proton)** with ultra-high dose rate, pulsed or continuous mode of operation.

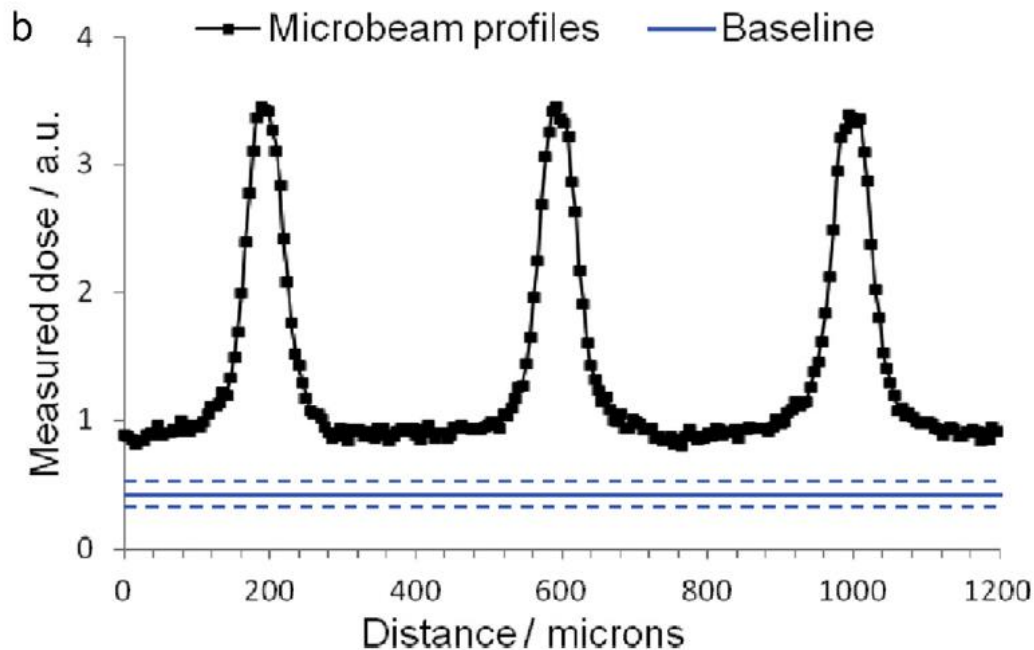


Microbeam radiation therapy (MRT)

Synchrotron-based MRT composed of spatially fractionated, planar x-ray (50-600keV) 25-75 micron-wide beams, with a very sharp penumbra, separated by a distance several times of their beam width.

These microbeams create unique dose profiles of alternating peaks and valleys with high peak-to-valley-dose-ratios (PVDR)

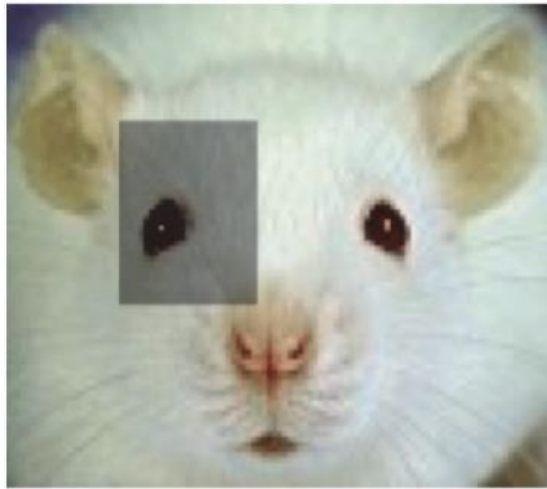
Zhang et al. *Expert Rev Anticancer Ther.* 2015 December



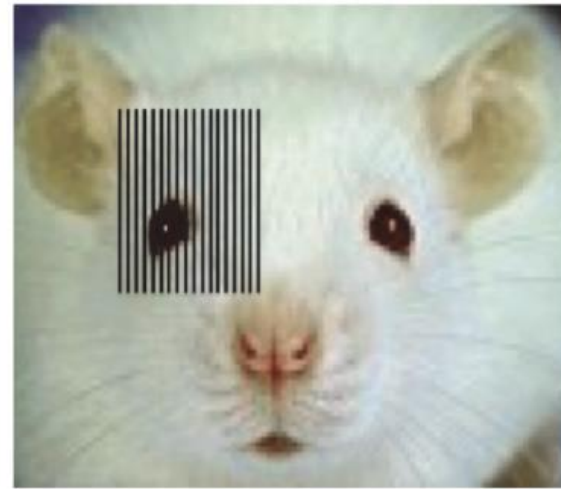
The highly brilliant Synchrotron sources have a very small beam divergence and an extremely high dose rate.

Peak entrance doses of several hundreds of Gy are extremely well tolerated by normal tissues and at the same time provide a higher therapeutic index for various tumor models in rodents.

E. Brauer-Krisch a, J-F.s Adam et al. Medical physics aspects of the synchrotron radiation therapies: Microbeam radiation therapy (MRT) and synchrotron stereotactic radiotherapy (SSRT) Physica Medica 31 (2015) 568e583



Synchrotron broad beam



Synchrotron microbeam

C. Fernandez-Palomo, C. Mothersill, E. Bräuer-Krisch, J. Laissue, C. Seymour, E. Schülke: γ -H2AX as a Marker for Dose Deposition in the Brain of Wistar Rats after Synchrotron Microbeam Radiation PLoS ONE 10(3): e0119924. 2015

Doses of 350 Gy can trigger the release of bystander signals that significantly amplify the DNA damage caused by radiation and that the γ -H2AX biomarker does not only represent DNA damage produced by radiation, but also damage caused by bystander effects.

Synchrotron-based MRT resulted in 10 fold prolonged survival of the treated animals with brain tumor xenograft

Donzelli *et al.*: Conformal image-guided MRT at the ESRF

With the implementation of conformal image-guided MRT, the treatment of deep-seated tumors in large animals will be possible for multiple port irradiations. The final workflow will consist of CT-imaging, subsequent individual treatment planning, including segmentation of target volume, organs at risk, and fiducial markers, and the definition of the treatment fields.

Physiologically gated microbeam radiation using a field emission x-ray source array

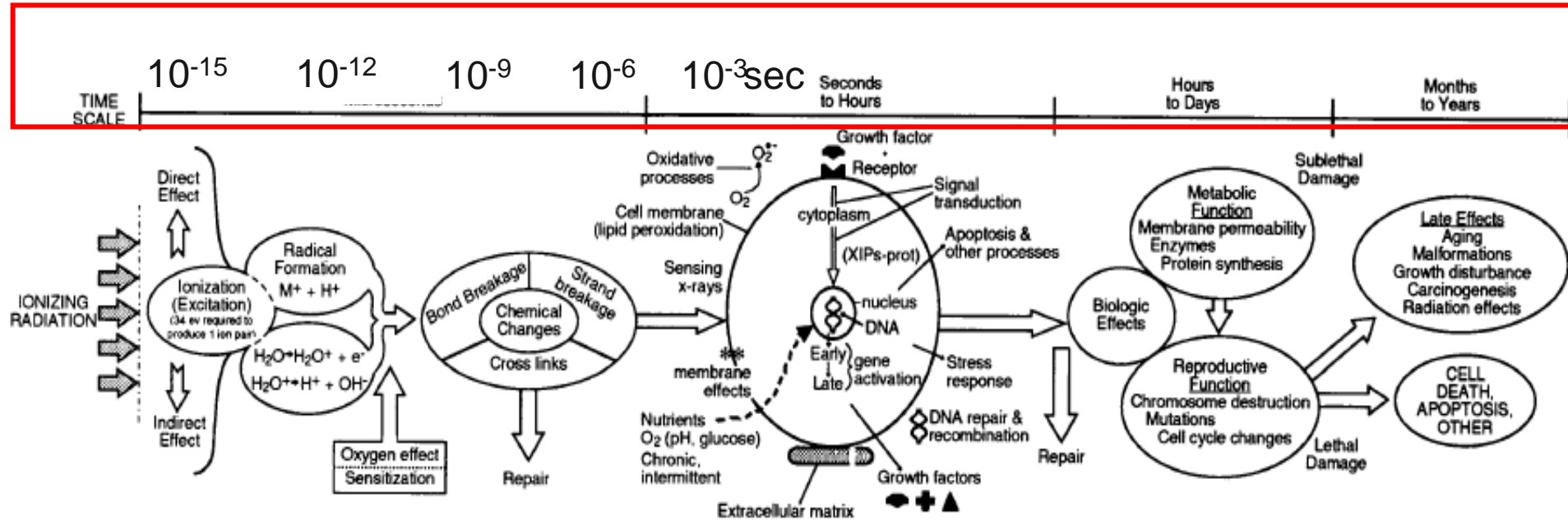
In the *in vivo* study, the histology result showed gating increased PVDR by a factor of 2.4 compared to the nongated case, similar to the result from the phantom study. The full width at tenth maximum of the microbeam decreased by 40% in gating *in vivo* and close to 38% with phantom studies.

The CNT field emission x-ray source array can be synchronized to physiological signals for gated delivery of x-ray radiation to minimize motion-induced beam blurring. The technique allows for more precise MRT treatments and makes the CNT MRT device practical for extended treatment.

Cell culture and in vivo tumor model experiments on pulsed mode



Time scale of RT effects



Radiobiological influence of megavoltage electron pulses of ultra-high pulse dose rate on normal tissue cells L. Laschinsky (10¹² Gy/min, <80 mGy/ 1ps)

Oppelt M, et al. (2015) Comparison study of in vivo dose response to laser-driven versus conventional electron beam. Radiat Environ Biophys 54:155–166

FLASH irradiation: <500ms pulses of >40 Gy/s

A 17 Gy conventional irradiation induced pulmonary fibrosis and activation of the TGF-beta cascade in 100% of the animals 24-36 weeks post-treatment, as expected, whereas no animal developed complications below 23 Gy flash irradiation, and a

30 Gy flash irradiation was required to induce the same extent of fibrosis as 17 Gy conventional irradiation.

*Favaudon V, Fouillade C, Vozenin MC **Ultra-high dose-rate, "flash" irradiation minimizes the side-effects of radiotherapy**] Cancer Radiother. 2015 Oct;19(6-7):526-31*

Laser driven particle beams

X-UV, X-ray
photons

Very high energy
electron

Protons
ions
neutrons

Integrated facility with particle selection?

Ultra short pulses

Ultra high dose rate ($<1\text{Gy/s}^{-10}$)

High repetition rate

Microbeams of photons (50-600 KeV) protons (20 MeV) ?

Laser driven ionizing radiation beyond VHEE and proton acceleration

Ultraintense beam

- short treatment time without increased entrance (skin) dose
- high temporal resolution (adaptive response, FLASH RT
 - Intensity modulation with higher resolution
 - Microbeam RT

Ultrashort dose delivery

- no need for internal organ motion management

Potential for simultaneous multiple particle beams

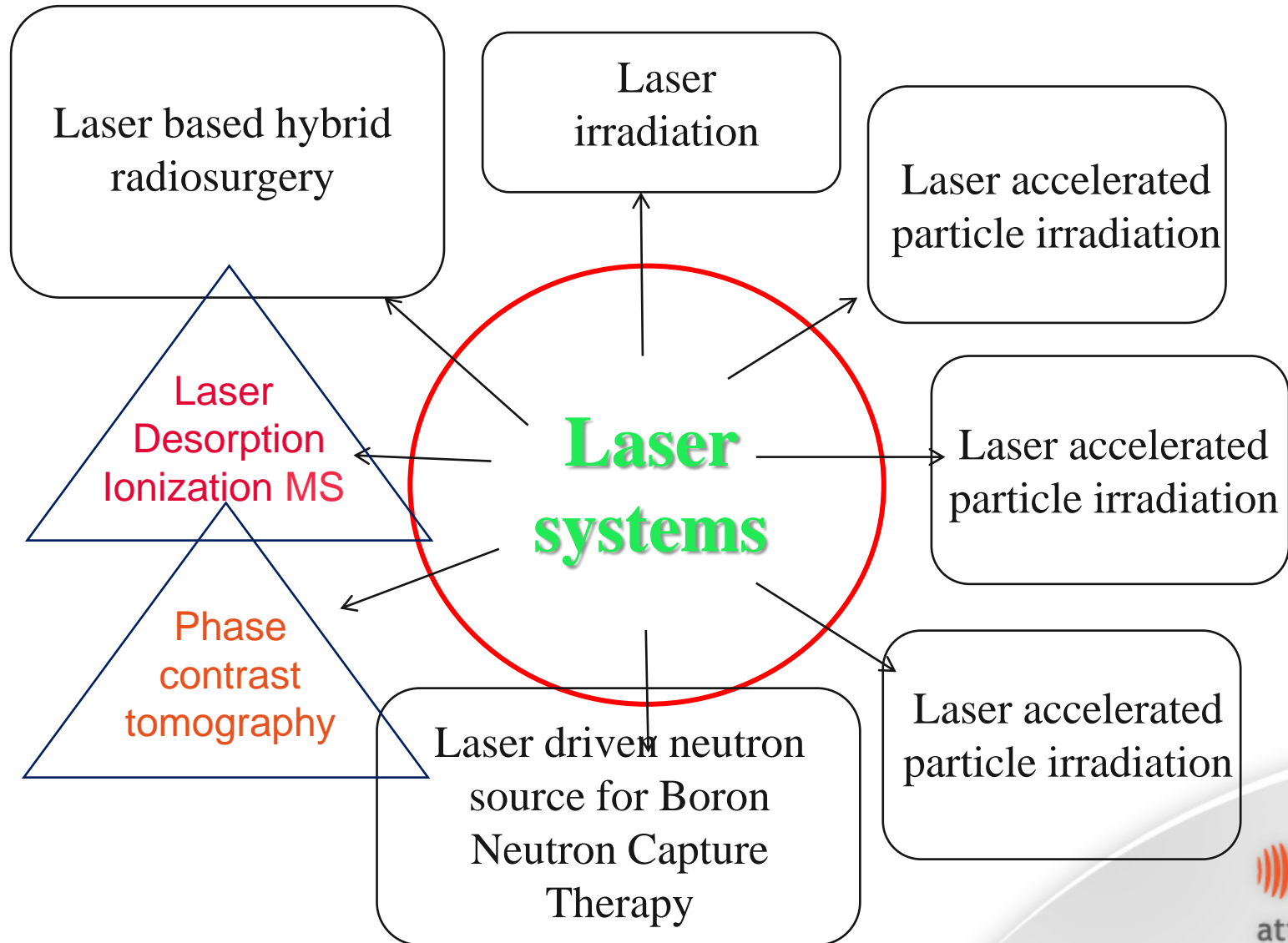
Epithermic neutron beam for BNCT

LET/RBE painting

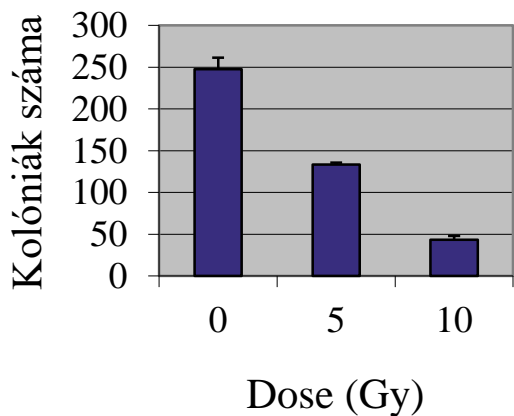
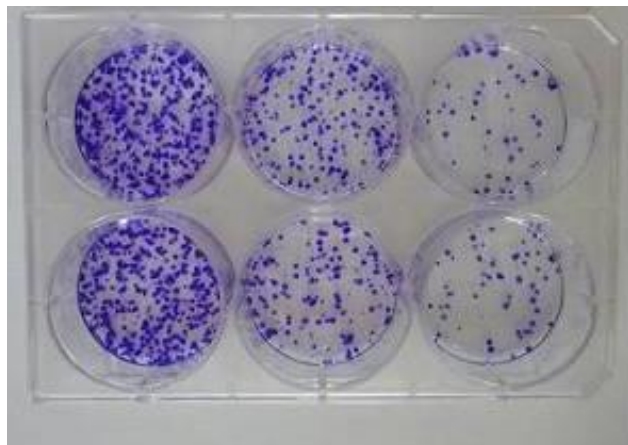
Flexibility

- intra operative radiotherapy – hybrid radio-surgery

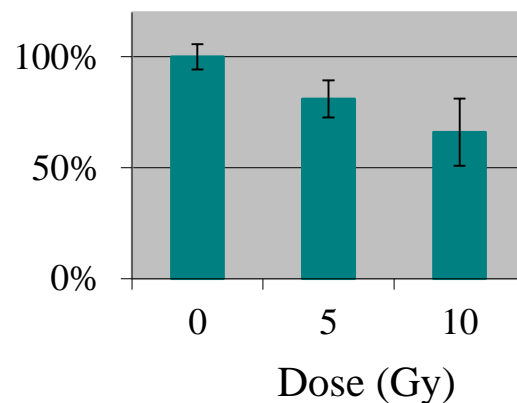
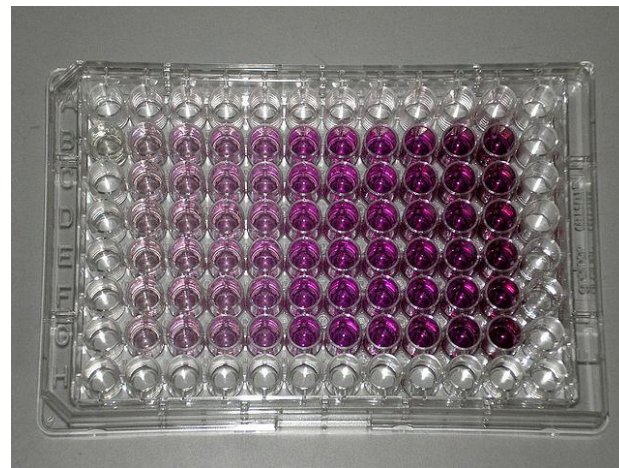
Hospital based complex Laser Facility for cancer treatment



Colony forming assay

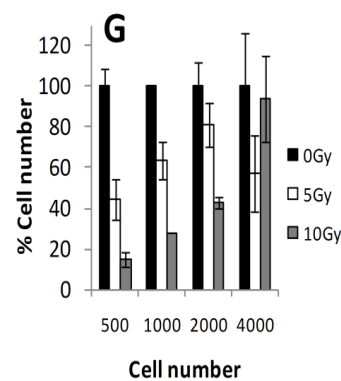
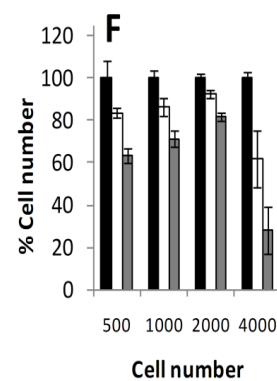
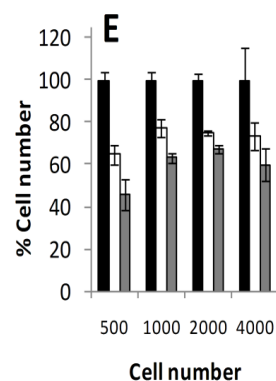
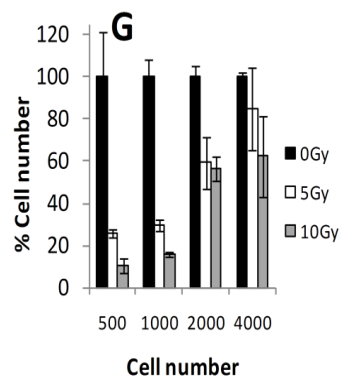
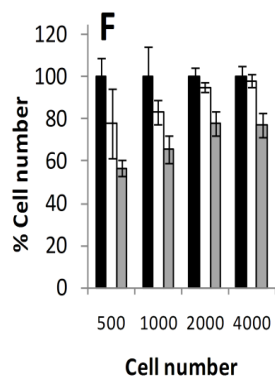
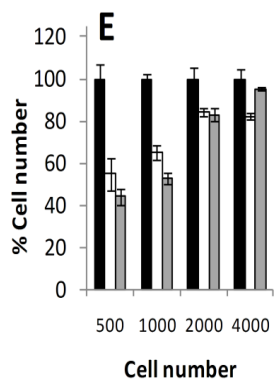
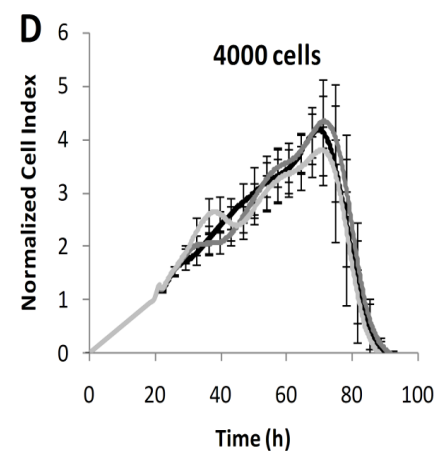
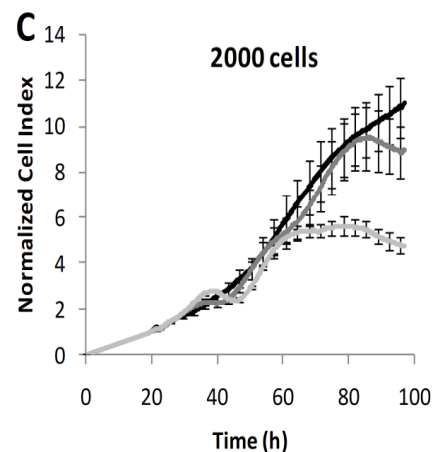
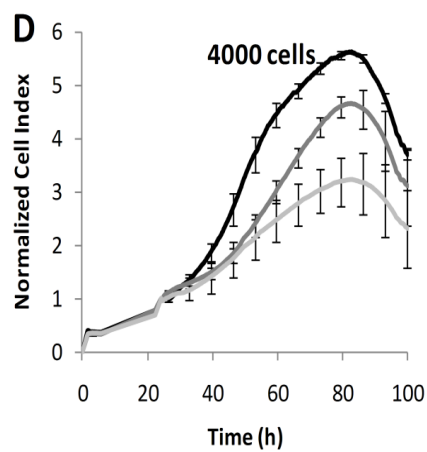
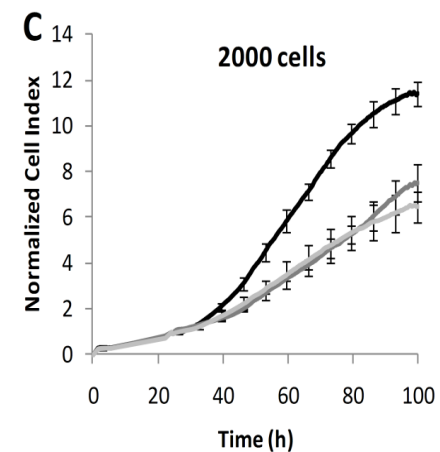
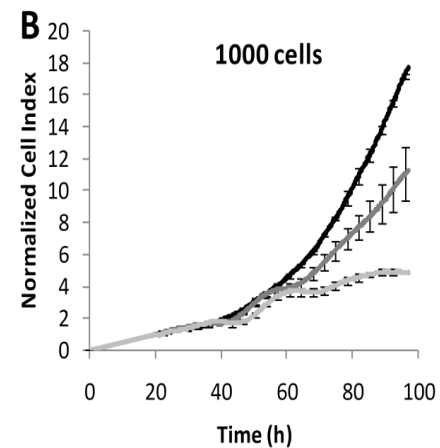
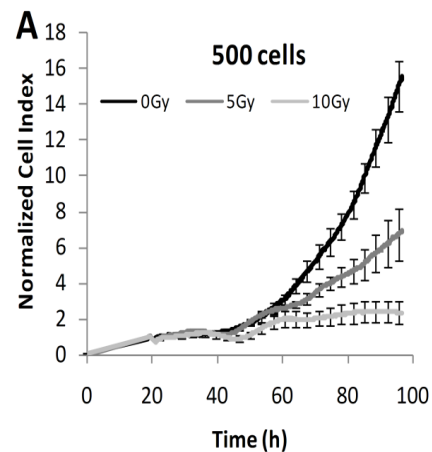
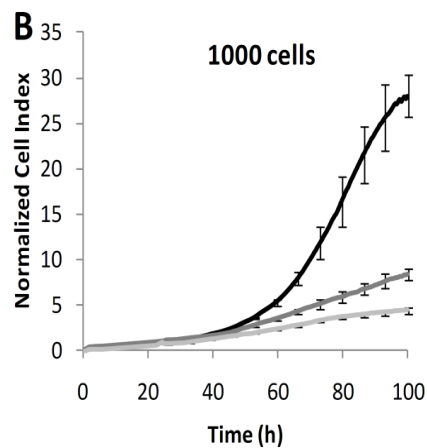
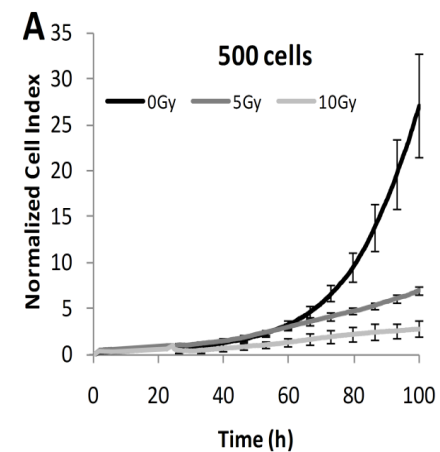


MTS assay



Dynamic monitoring of ionizing radiation effect using a Novel Real-Time Cell Analysis Platform

Mán I, Plangár I, Szabó ER, Tőkés T, Szabó Z, Nagy Z, Fekete G, Mózes P, Puskás LG, Hideghéty K, Hackler L Jr



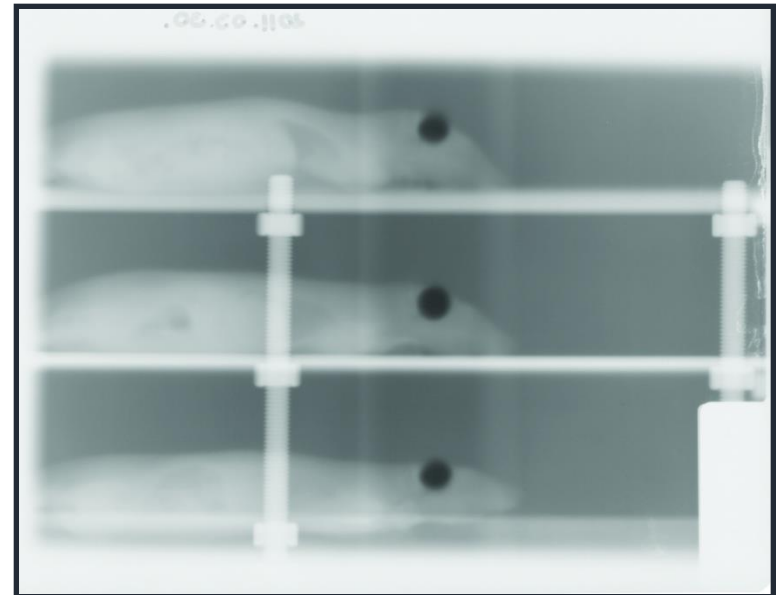
Anaesthesia: i.p. chloral-hydrate

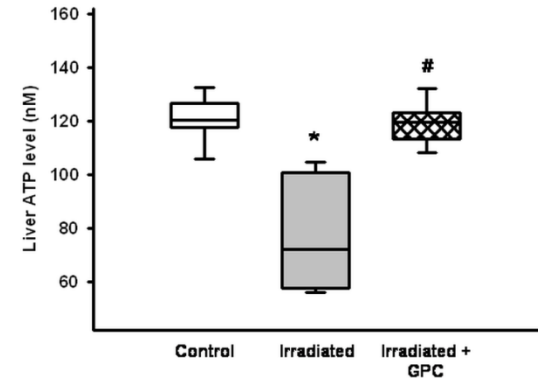
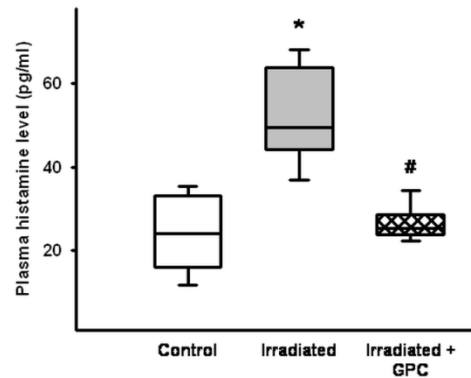
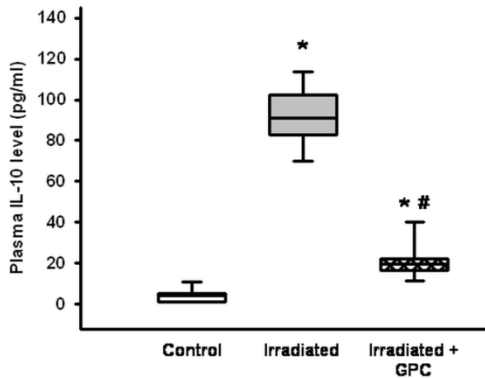
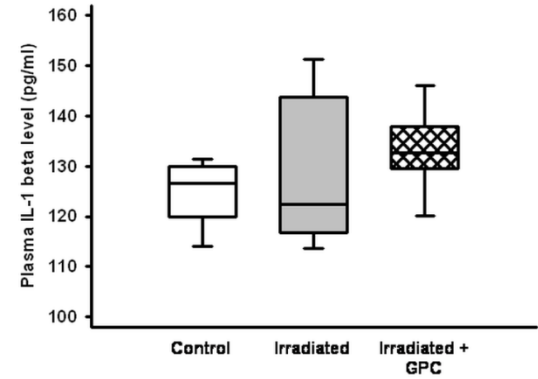
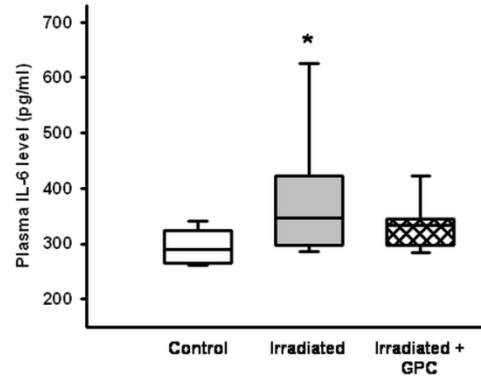
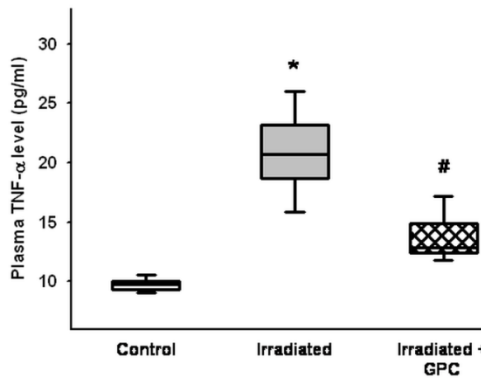
Positioning: special bunk-bed

Source: 1,26 MeV energy Cobalt

Dose: 40 Gy (2x20Gy)

Irradiation: 10 mm diameter collimator, homogen irradiation of hippocampus
(at both hemispheres)





Statistics: Between groups: Kruskal-Wallis and Dunn-test
 (Median, 25th and 75th percentiles) * $p < 0.05$ vs Control group, # $p < 0.05$ vs Irradiated group.

- * There are significant production of pro- and anti-inflammatory cytokines (TNF- α , IL-6, IL-10) after 40 Gy hippocampal irradiation in the brain.
- * Therefore the BBB opens and the inflammatory cytokines appear in the peripheral circulation.

At the same time,

i.v. GPC treatment prevents:

- the ATP depletion,
- the elevation of the histamine and the pro-inflammatory cytokine (TNF- α and IL-6) levels,
- increase the anti-inflammatory cytokine (IL-10) level

The exogen GPC has anti-inflammatory effect and provide protection against the irradiation-induced brain inflammation caused biochemical consequences.

Chronic project: Methods

„Radio-neuroprotective effect of L-alpha-glycerolphosphorylcholine in experimental rat model”



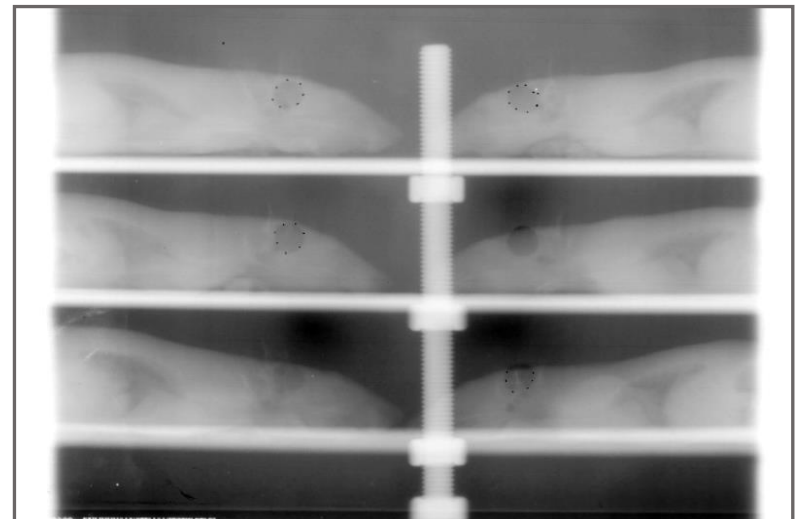
Anaesthesia: i.p. chloral-hydrate

Positioning: special bunk-bed

Source: 6 MeV energy Siemens linear accelerator

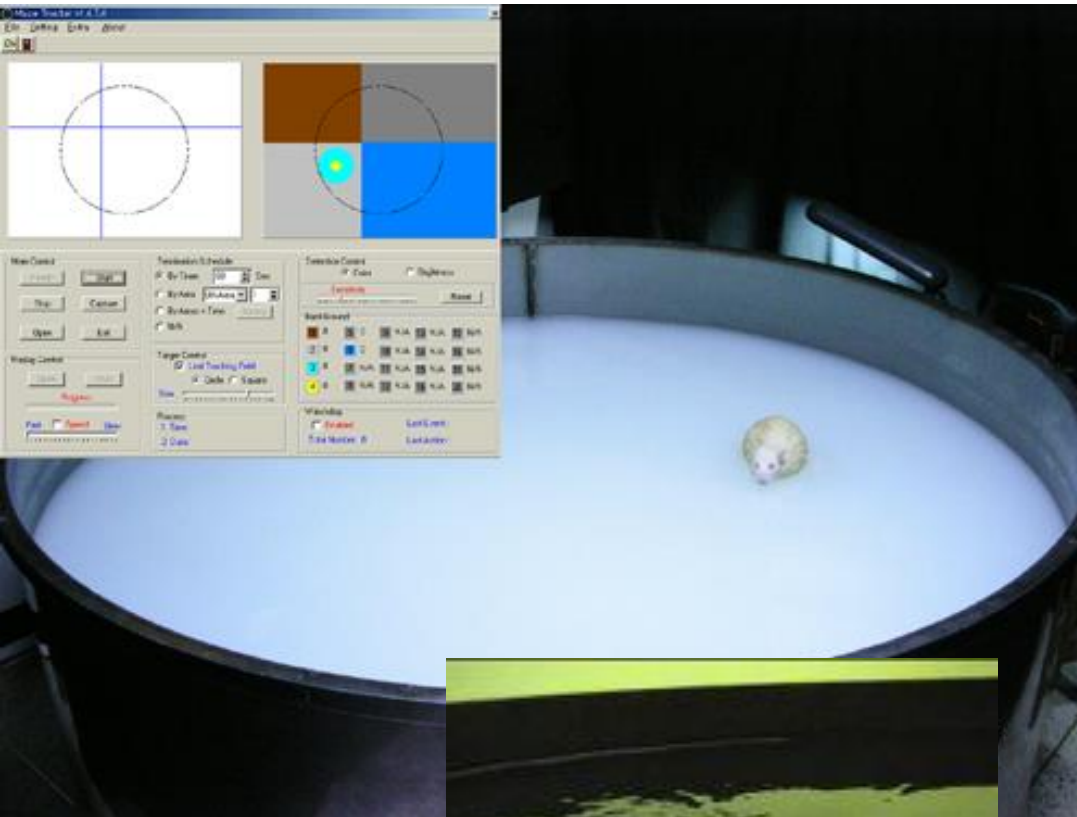
Dose: 40 Gy

Irradiation: 10 mm diameter collimator, homogen irradiation of hippocampus (at one hemisphere)

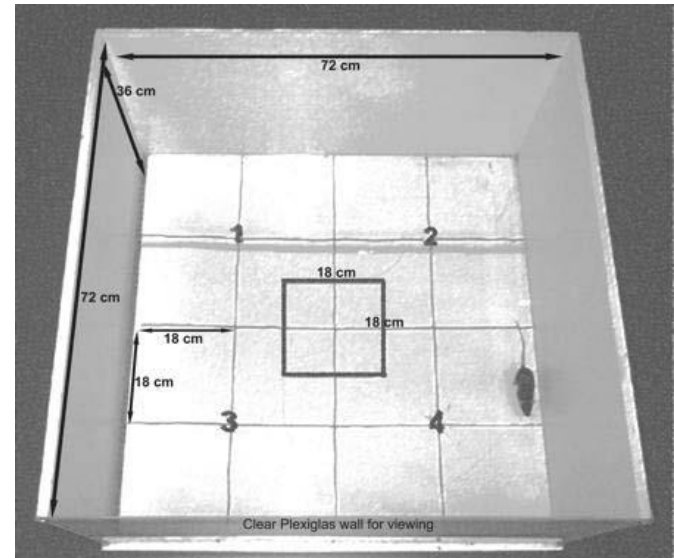


Neurofunctional tests

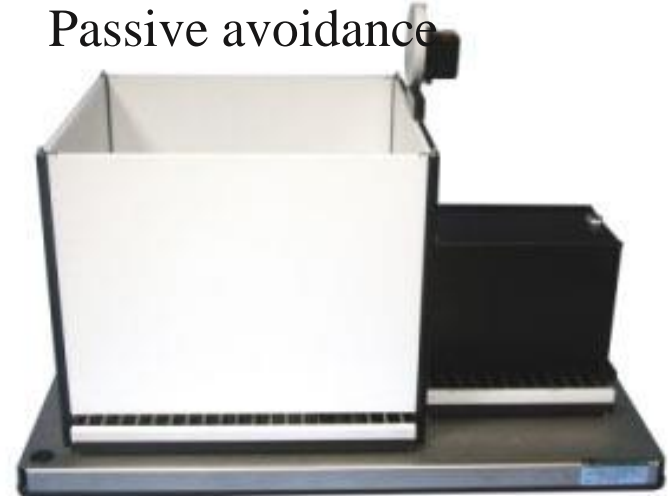
Morris Water maze



Open-field test

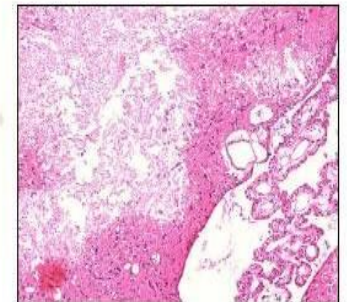


Passive avoidance



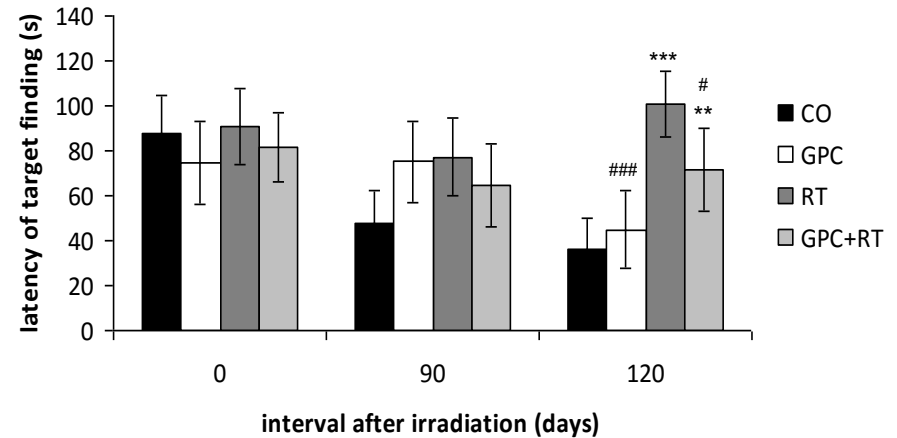
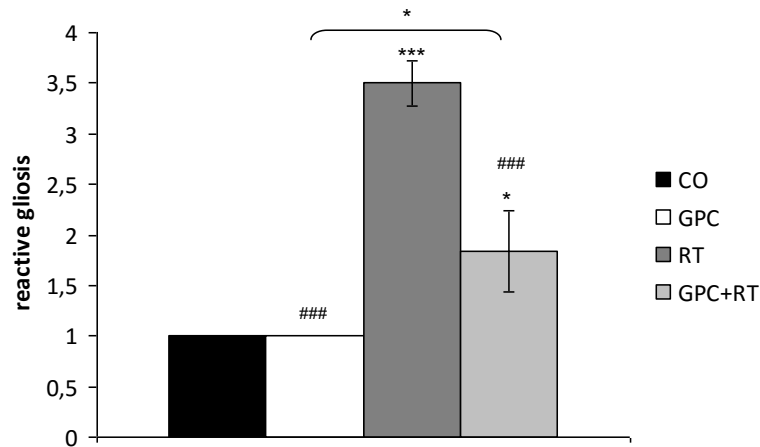
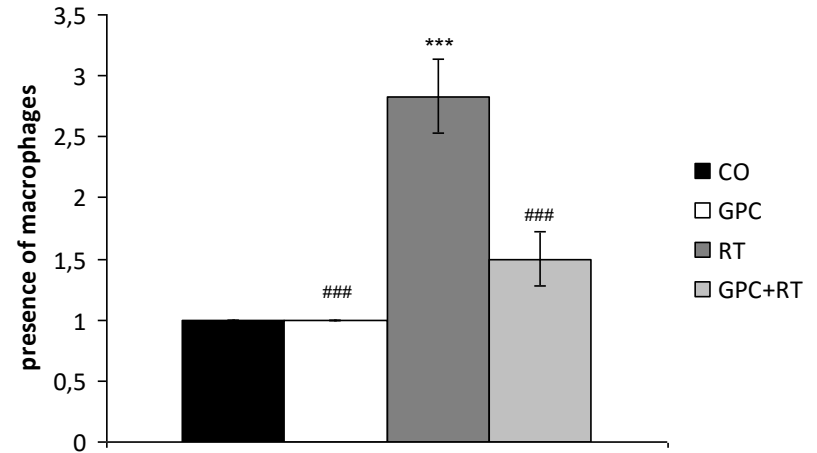
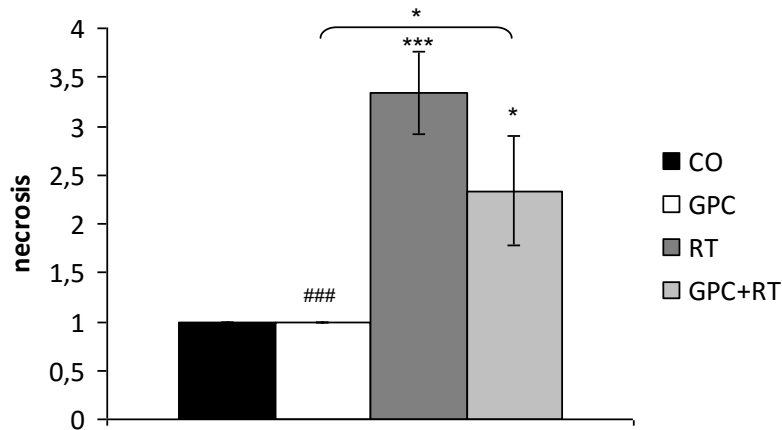


Late effects of focal brain irradiation



Chronic project: Results

„Radio-neuroprotective effect of L-alpha-glycerolphosphorylcholine in experimental rat model”



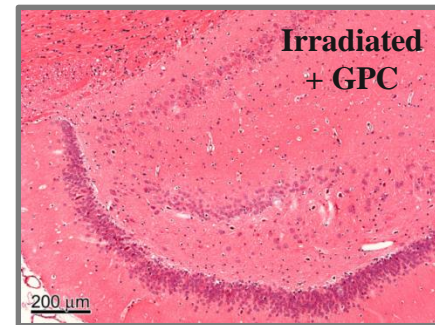
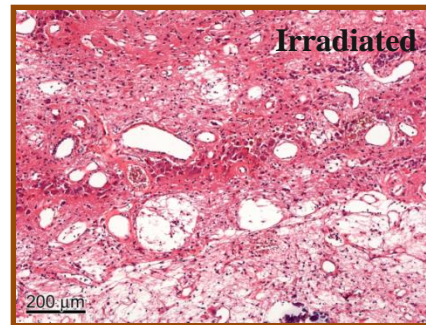
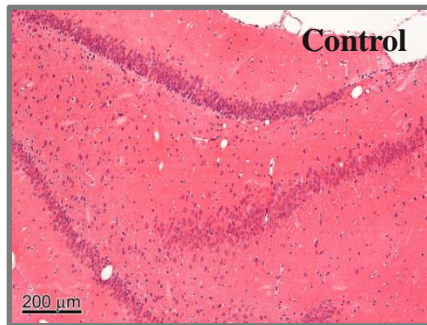
Statistics: Kruskal-Wallis, Fisher's PLSD (mean \pm S.E.M.) * $p < 0.05$ vs Control group, # $p < 0.05$ vs Irradiated group.

Chronic project: Summary

„Radio-neuroprotective effect of L-alpha-glycerolphosphorylcholine in experimental rat model”



The morphological changes in the irradiated brain tissue (significant macrophage accumulation, the levels of the reactive gliosis, calcification and demyelination) were reversed by the 4-month oral GPC treatment.



Significant functional and morphological changes were observed four months after 40 Gy single dose brain irradiation. GPC supplementation provided significant protection against cognitive disturbances and cellular damages.

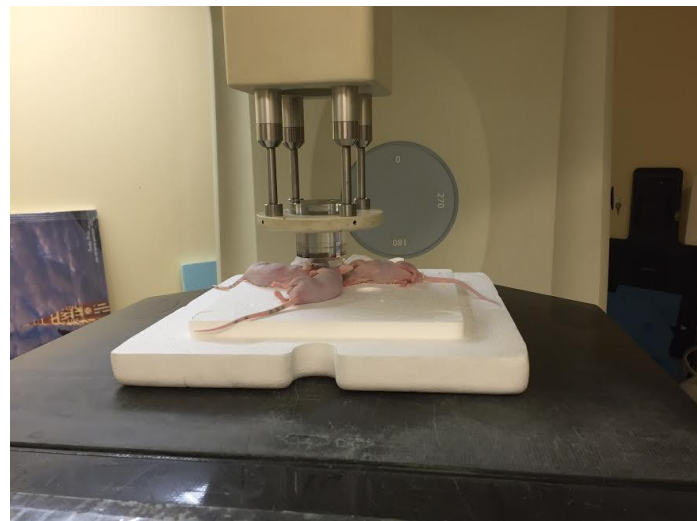
Anaesthesia: i.p. chloral-hydrate

Positioning: on one side

Source: 6 MeV energy Siemens linear accelerator

Dose: 40 Gy

Irradiation: 5 mm diameter collimator



Novel vertebrate model for radiobiology



Zebrafish (*Danio rerio*):

- Easy to handle, good reproduction captivity,
- transparent in larval stages
- external fertilization, rapid embryonic development,
- the complete genome sequence was published (2013)
- Availability of several transgenic lines

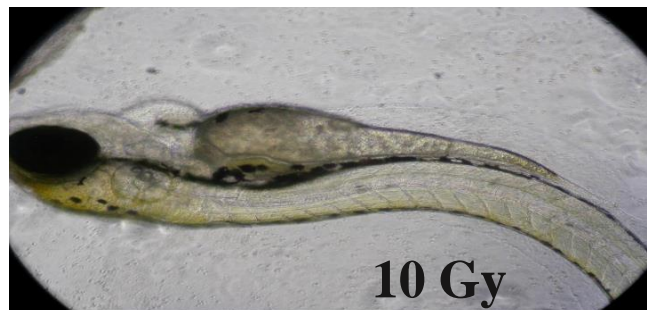
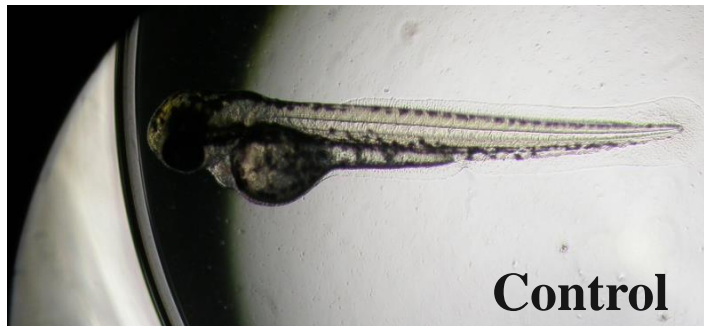
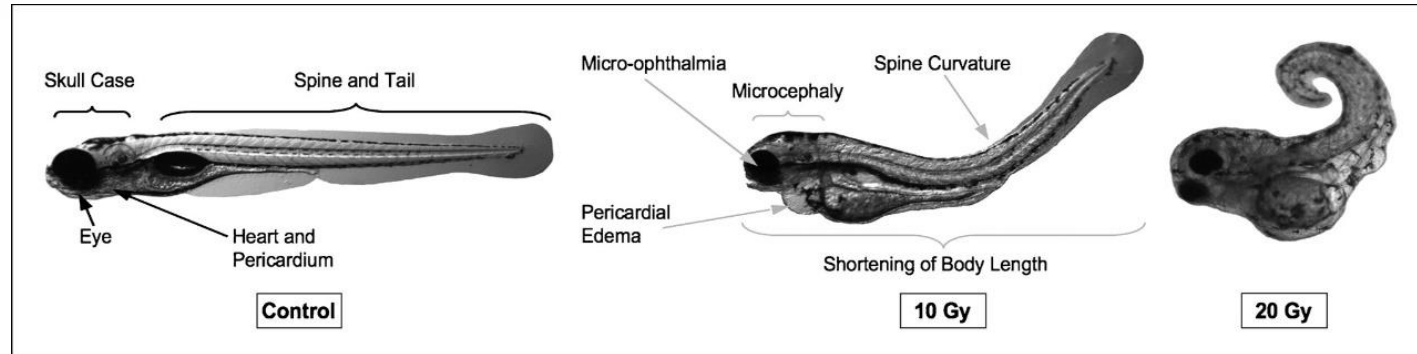


- **research fields:** radiobiology, melanoma, leukemia, pancreatic cancer, hepatocellular carcinoma, blood coagulation, heart failure, congenital heart and kidney defects, acute inflammation, retinal damage, teratology, biotechnological-, environmental protection-, toxicological- and pharmacological investigations.



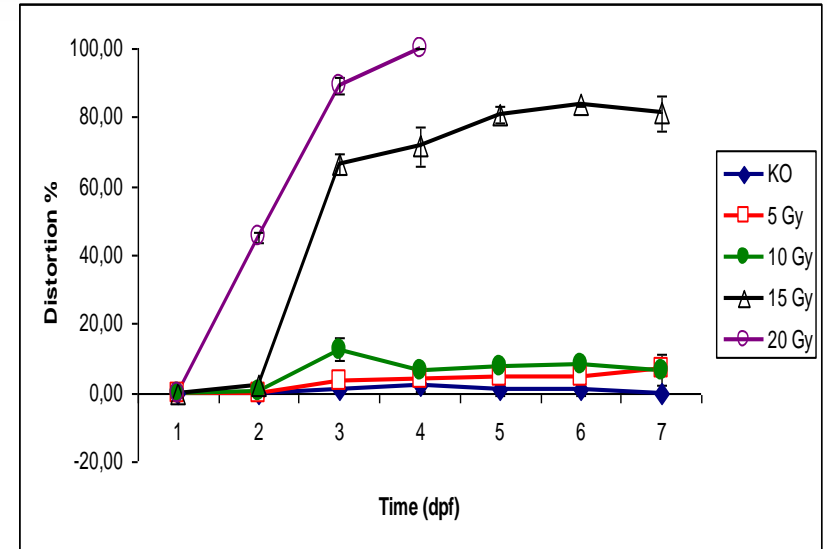
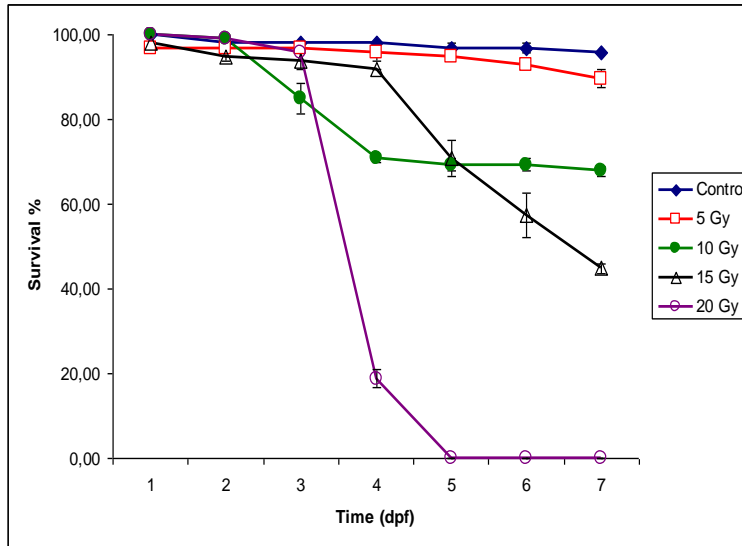
End points of zebrafish embryo experiments

detection of malformation and survival

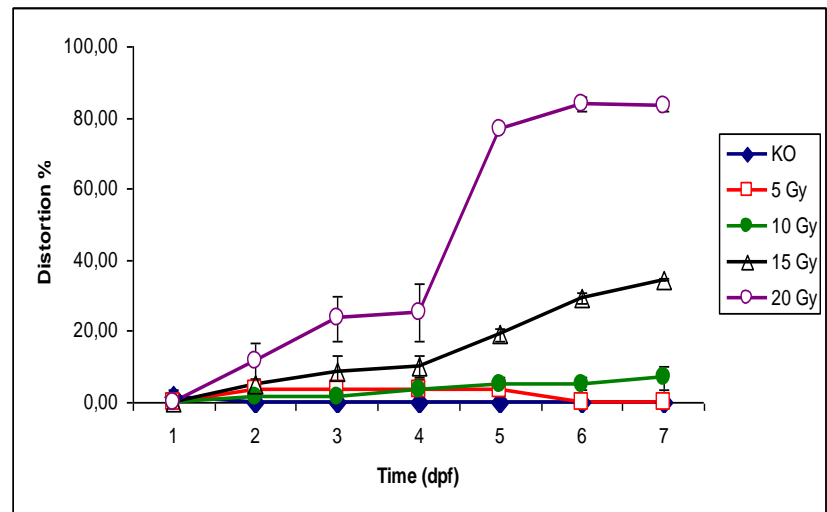
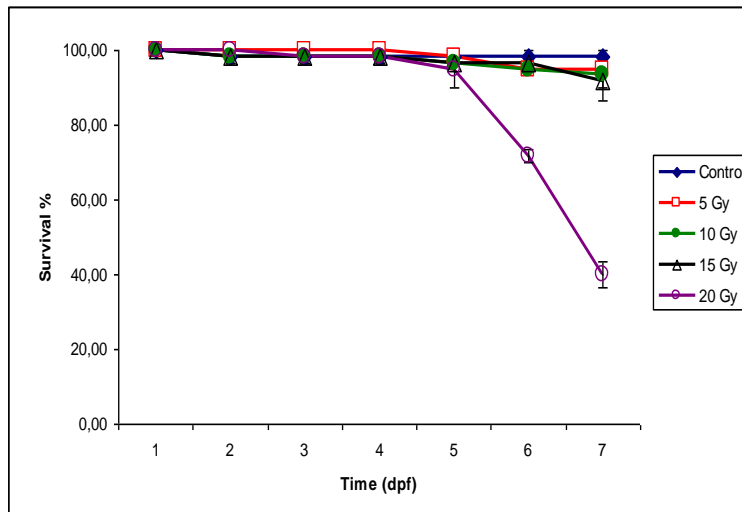


Results of the zebrafish embryos experiments

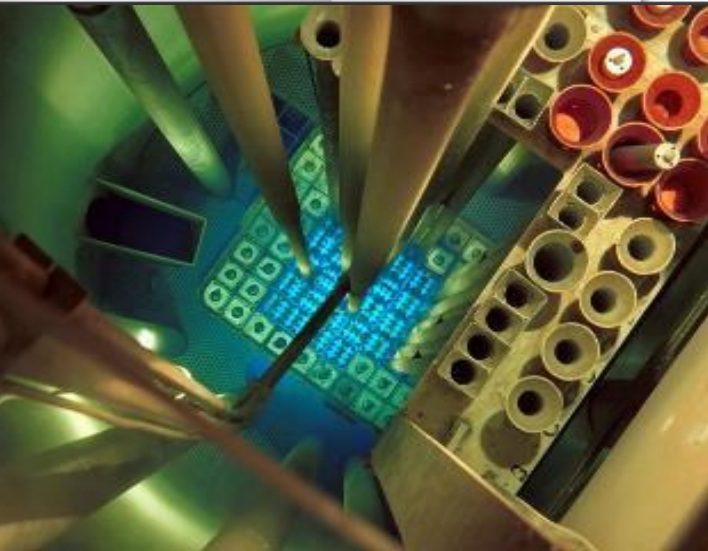
6 hpf



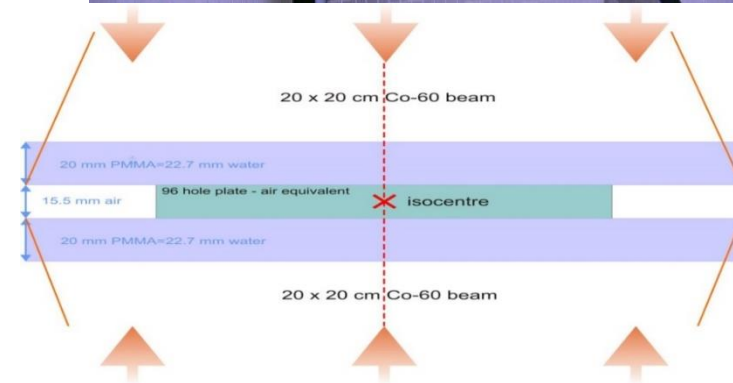
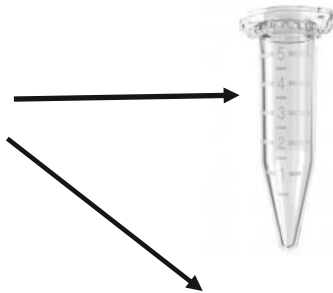
24 hpf



Irradiation of zebrafish embryos

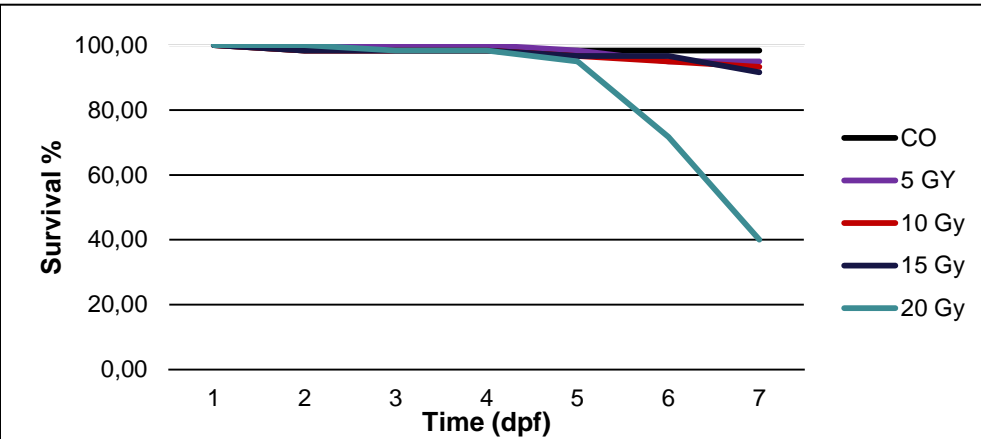


Wild type zebrafish embryos (24 hpf) were irradiated with photons at 5 - 20 Gy dose and reactor/cyclotron neutron-photon mixed beam at 1-8 Gy dose

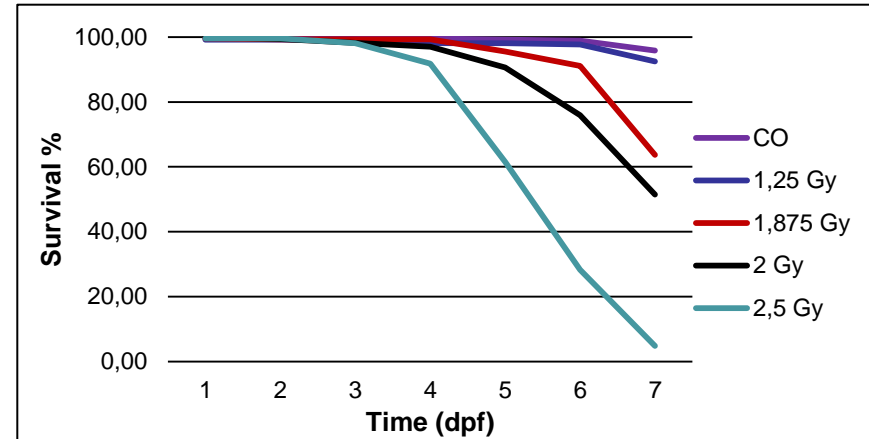


Results of the zebrafish embryos experiments

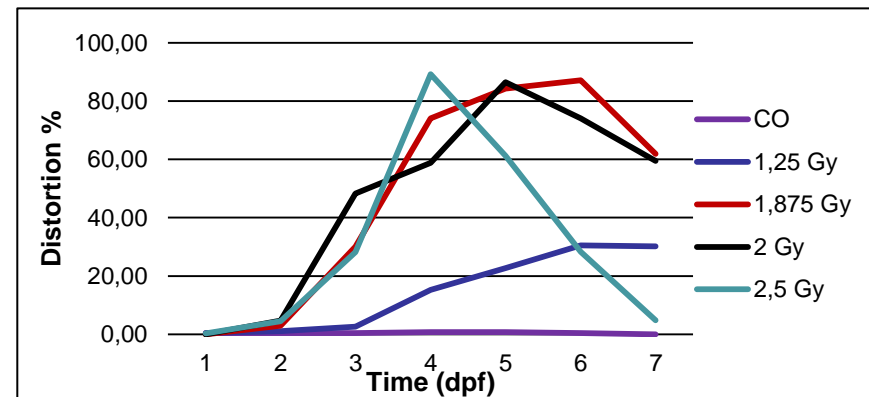
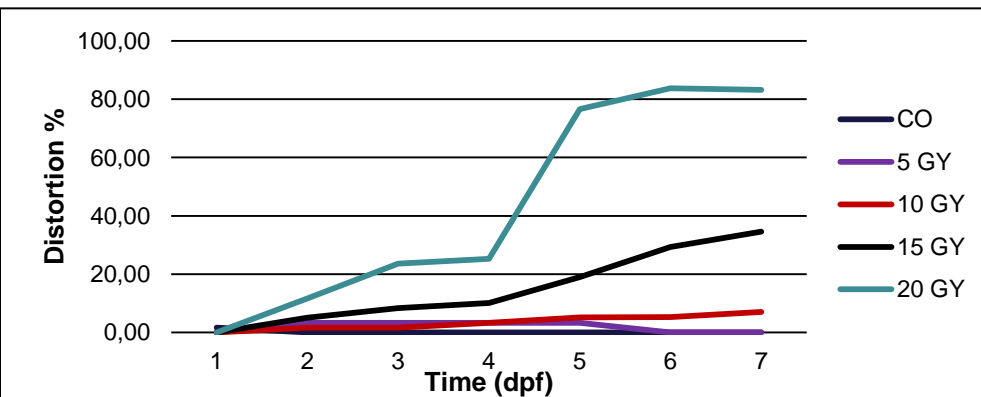
Photon



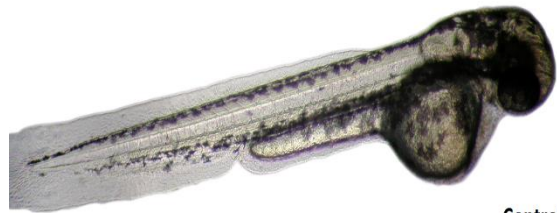
Neutron



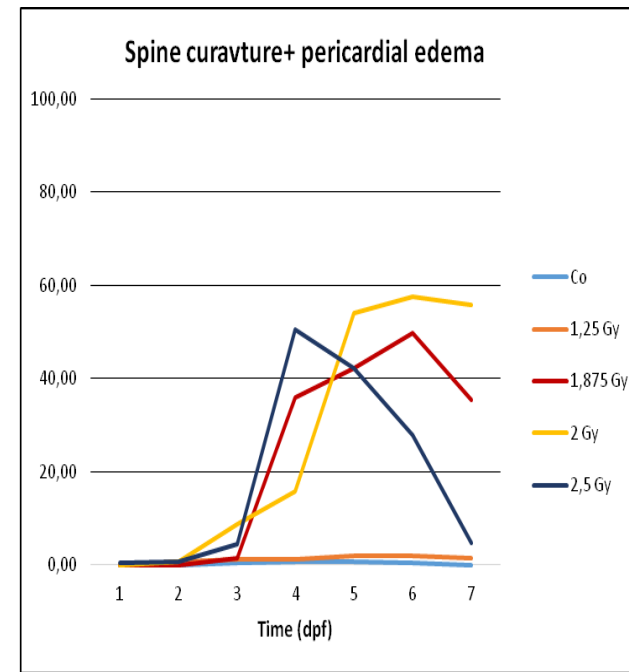
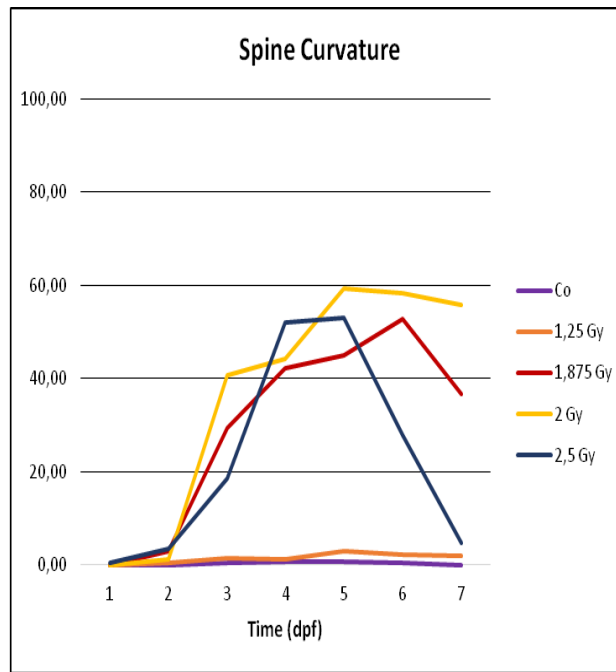
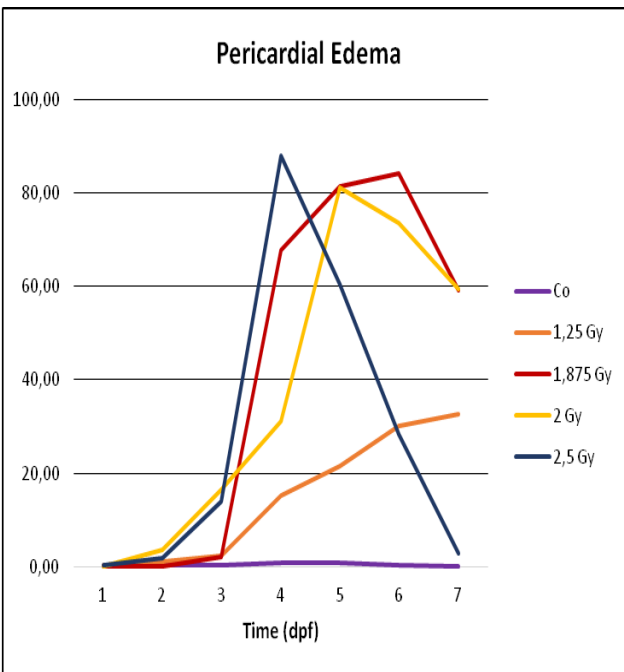
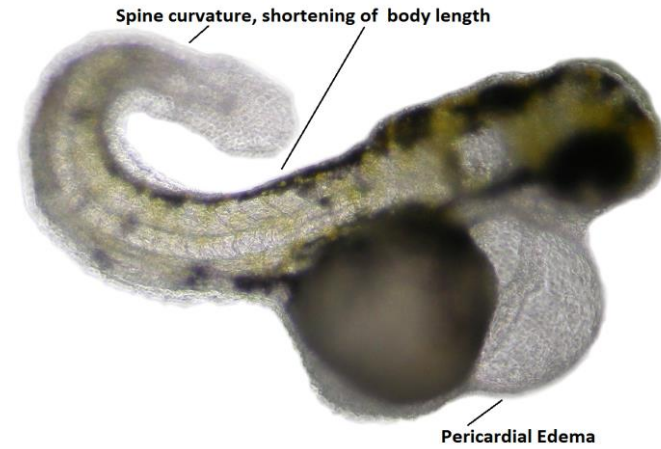
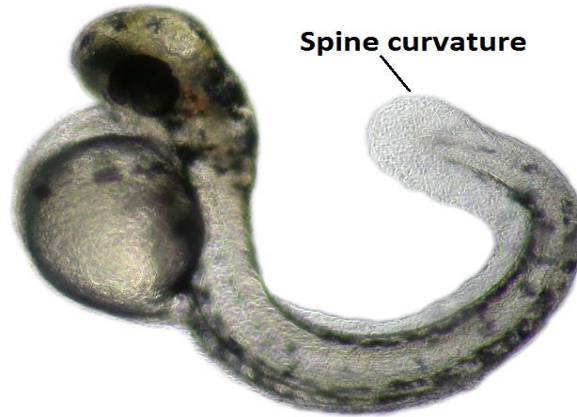
- $RBE = LD_{50ph} / LD_{50n} = 20 / 2 = 10$



Macroscopic morphological abnormalities of the zebrafish embryos



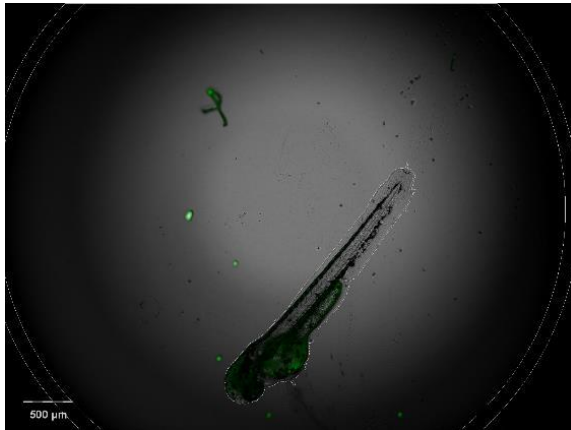
Control



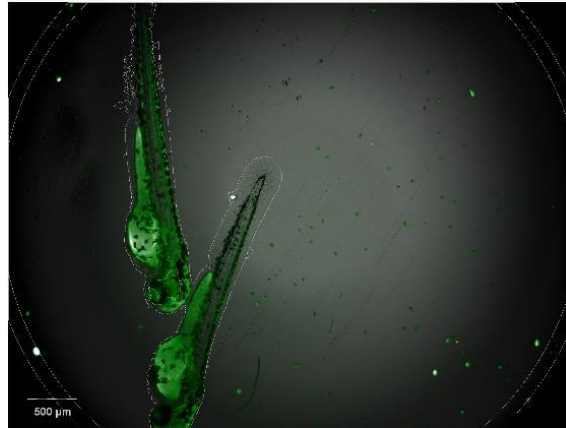
Imagig of neuron and blood vessel labeled transgenic zebrafish embryos



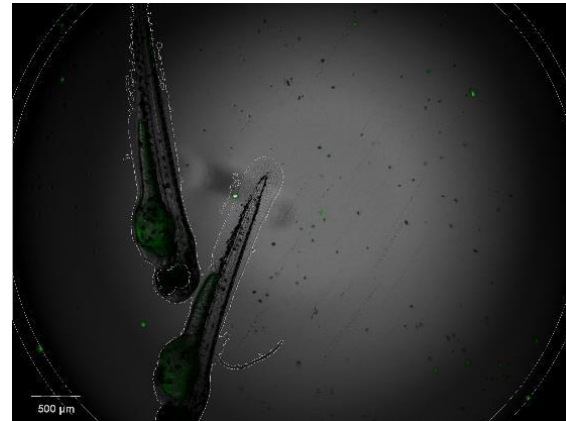
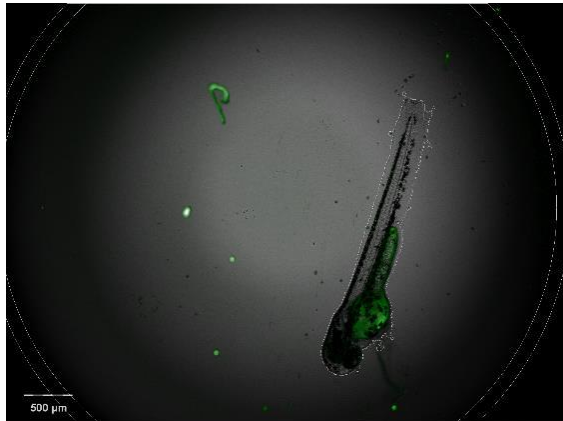
Confluency: 5.2
Signal GFP: 165
Signal dsRED: 65



Confluency: 10.7%
Signal GFP: 164
Signal dsRED: 65



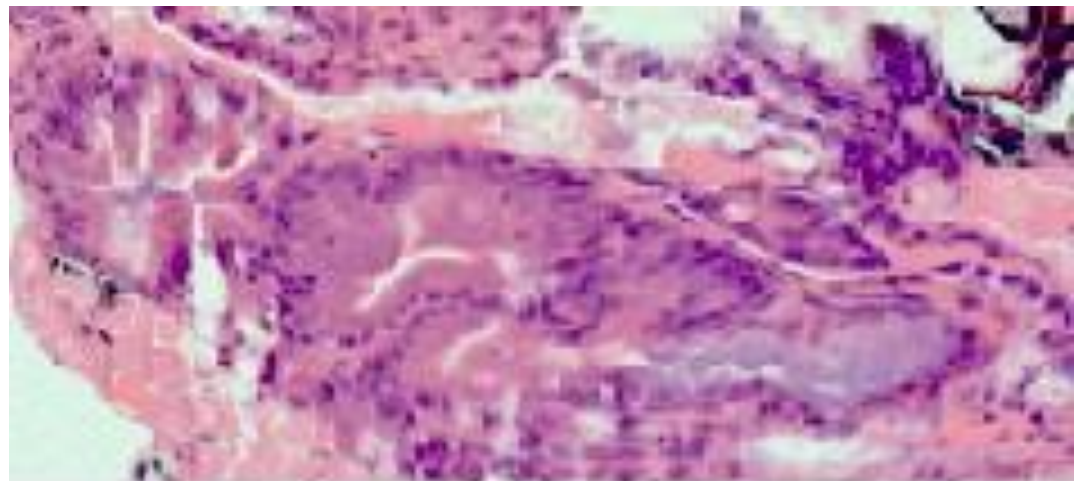
Confluency: 12.0
Signal GFP: 170
Signal dsRED: 65



Microscopic lesions of the zebrafish embryos



Control



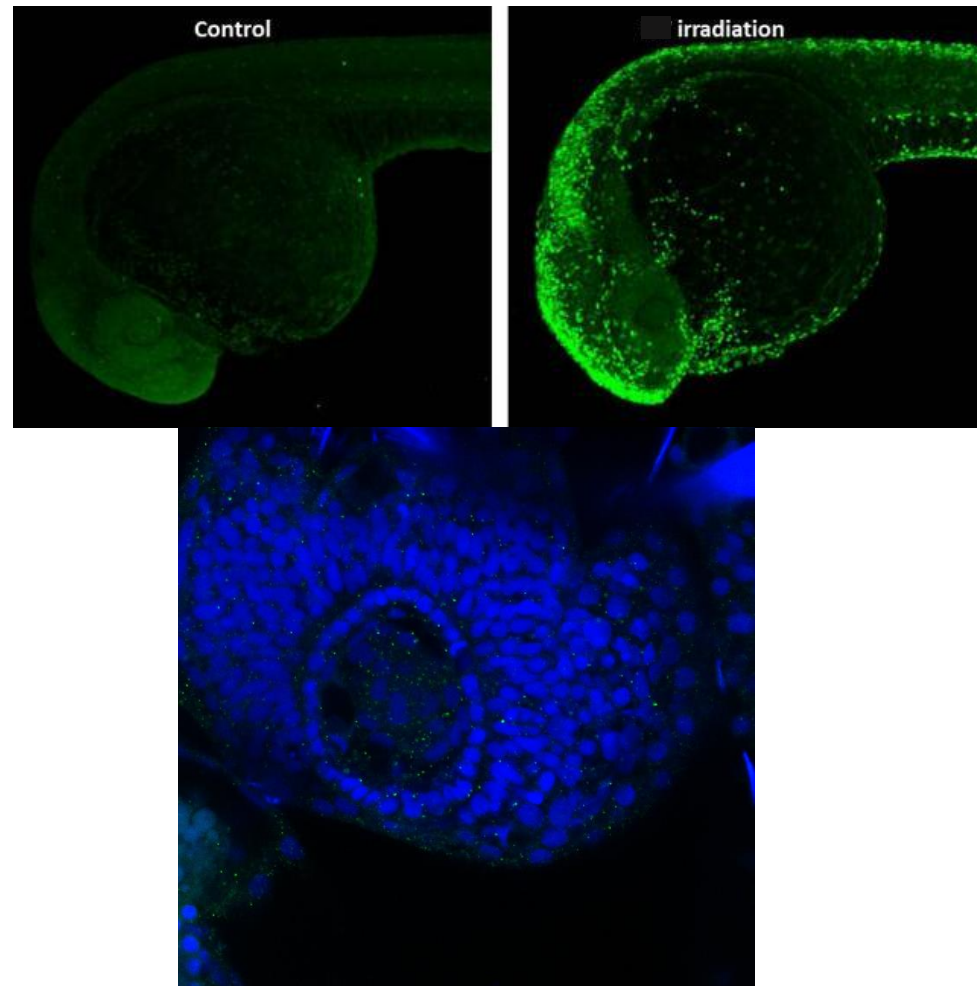
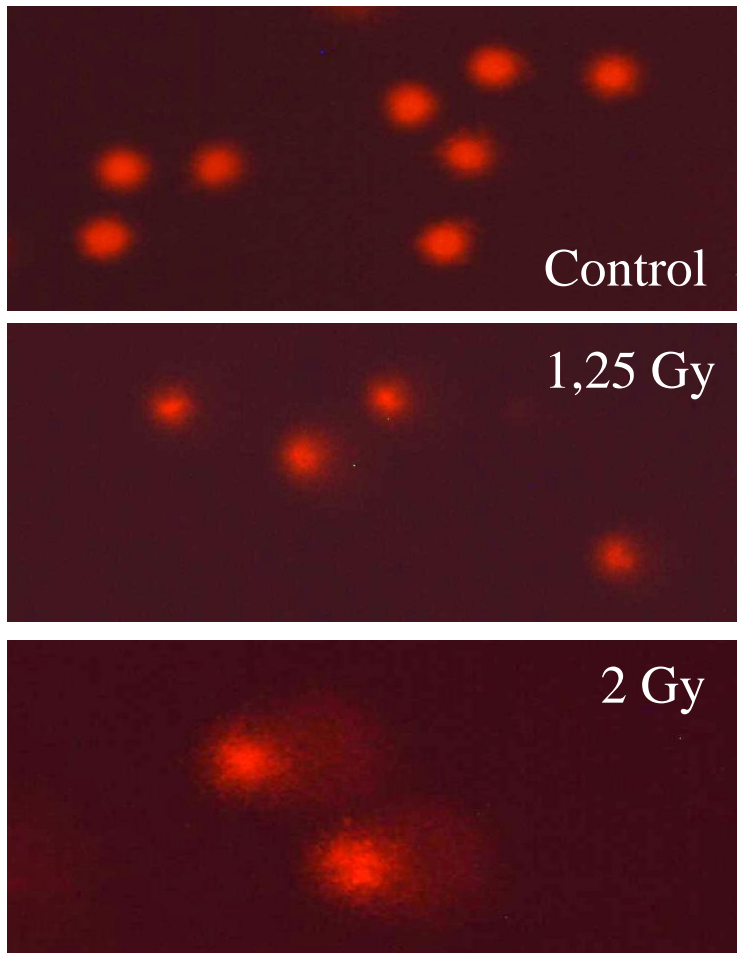
After 10 Gy

single strand breakes (SSB)

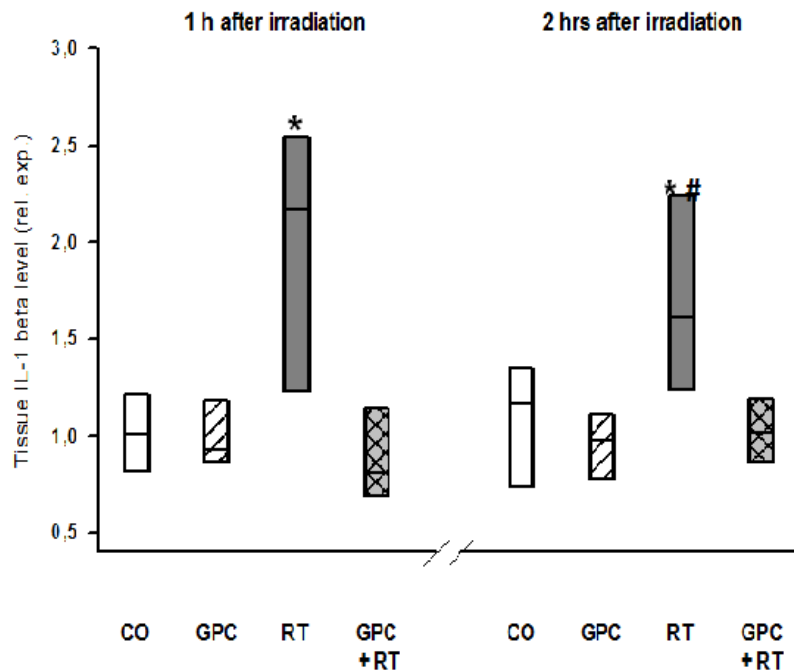
double strand breaks (DSB)

Comet assay

γ H2AX

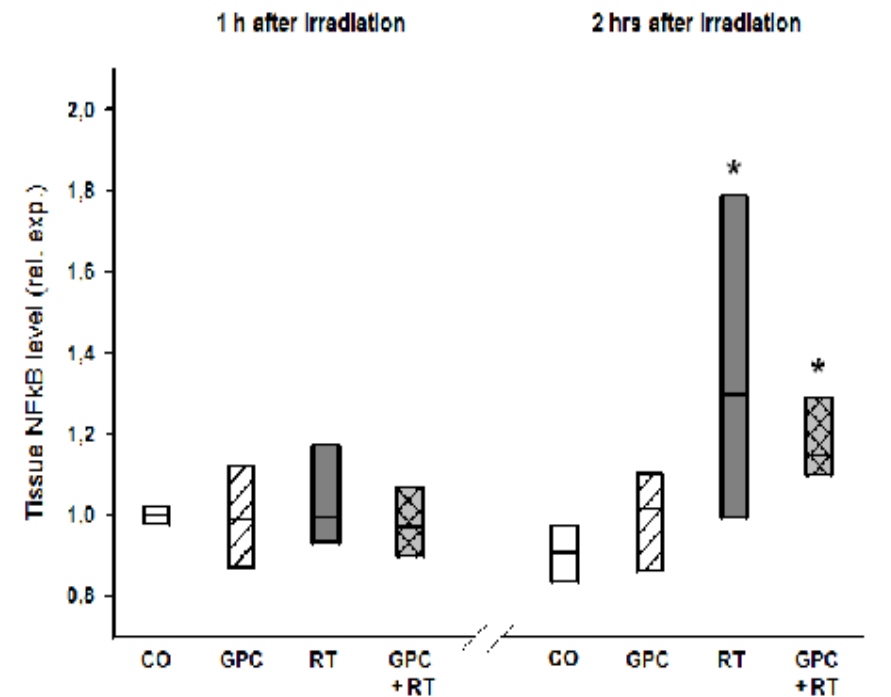


Tissue interleukin-1 β levels



*p<0,05 vs GPC + RT
#p<0,05 vs GPC

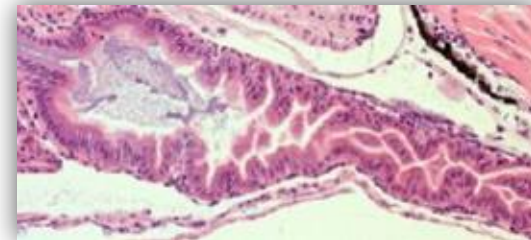
Tissue NF κ B levels



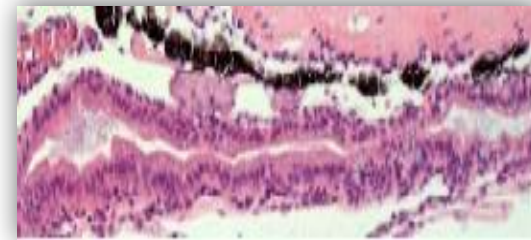
*p<0,05 vs Control

L-alpha glycerylphosphorylcholine (GPC)

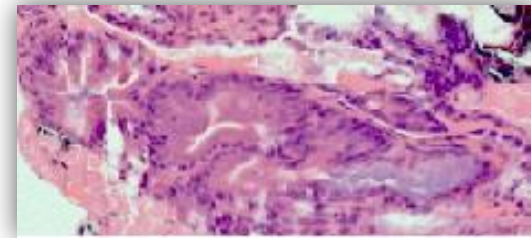
- deacilated derivative of phosphatidylcholine,
- phospholipid precursor,
- water-soluble,
- protective in stroke and in transient ischemic attack,
- anti-inflammatory effects,
- ROS scavenger.



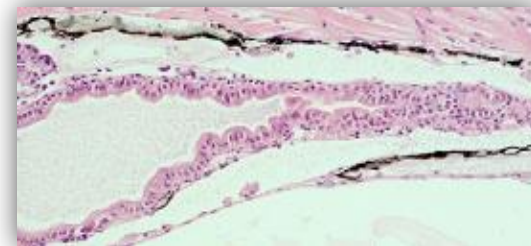
Control



GPC



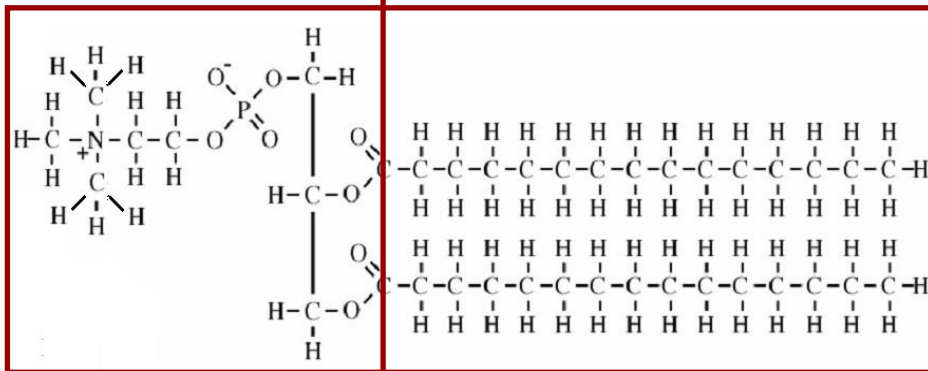
RT



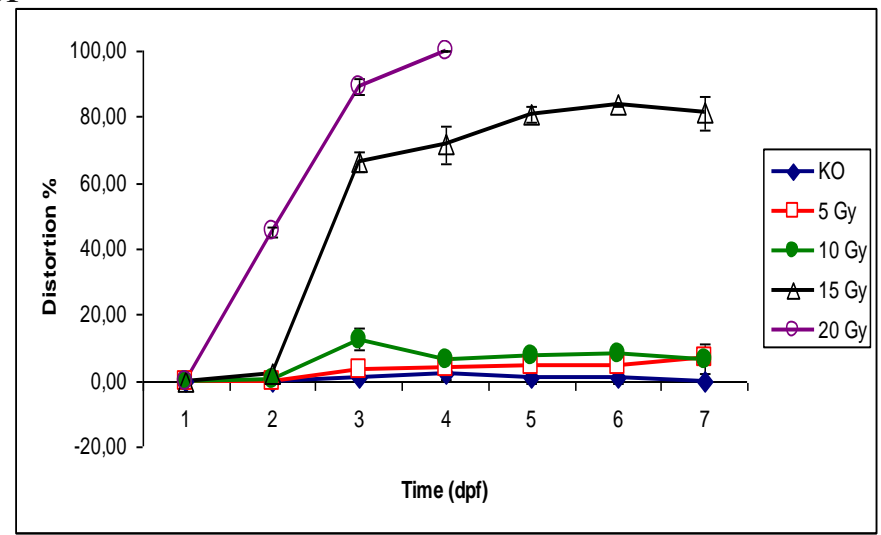
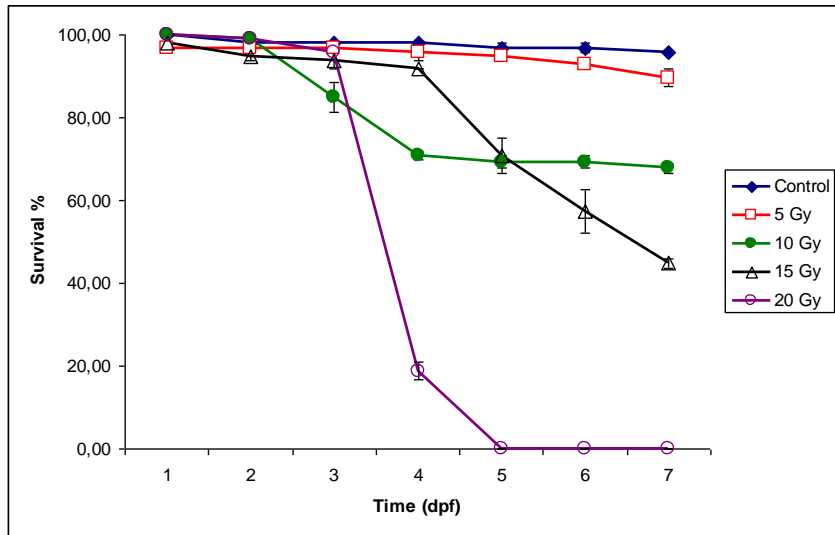
GPC + RT

Polar head group (choline)

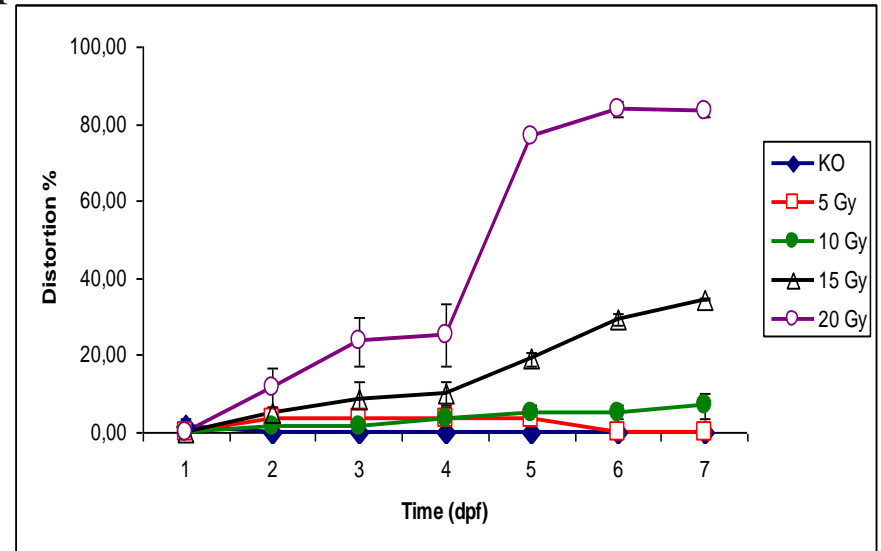
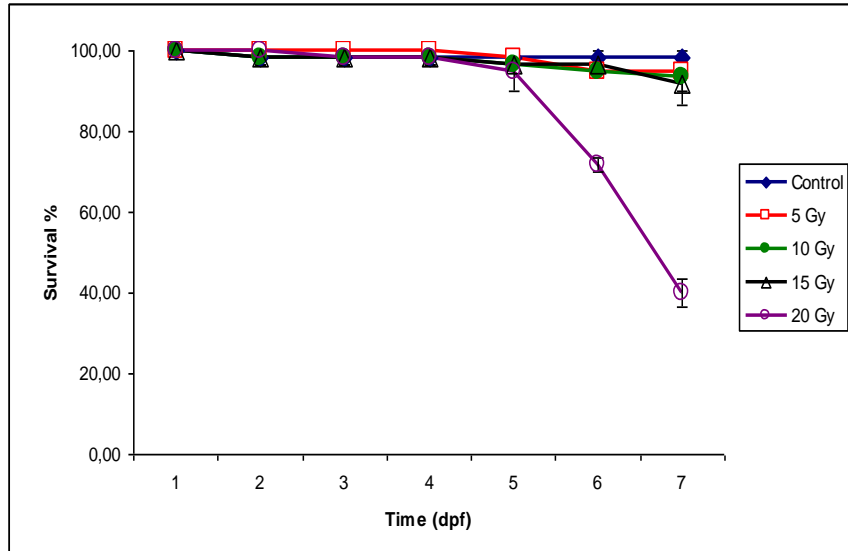
Apolar tail group (fatty acids)



6 hpf



24 hpf



Testing of the potential radioprotective agent L-alpha glycerylphosphoryl-choline in a zebrafish embryo model Szabó ER, Plangár I, Mán I, Daróczy B, Tókécs T, Szabó Z, Fekete G, Kovács R, Baska F, Boros M, Hideghéty 2016 Zebrafish Res.

Study design

After validation of ZF model with standard *in vitro* and *in vivo* biologic systems wild, and tissue-specific fluorescent labelled, embryos will be irradiated at different centers for cross comparison of biological effect of laser accelerated ion beams.

1hpf embryos will be exposed to laser driven protons at 0, 2, 4, 8, 16 Gy dose level positioned in 1 mm-steps in 3 plastic bags from 0-3 mm at different laser driven proton facility.

Endpoints:

- survival- definition of RBE, alpha/beta values
- organ development deterioration
- tissues changes of different organs (eye, heart, bowel, liver)
- gammaH2AX staining 30 minutes after RT and 72 hours after
- frozen samples for further molbiol studies

Energy [MeV]	Proton range in water [mm]
5	0,36
8	0,8 ?
10	1,2



**THANK YOU
FOR YOUR
ATTENTION!**

SZÉCHENYI 2020

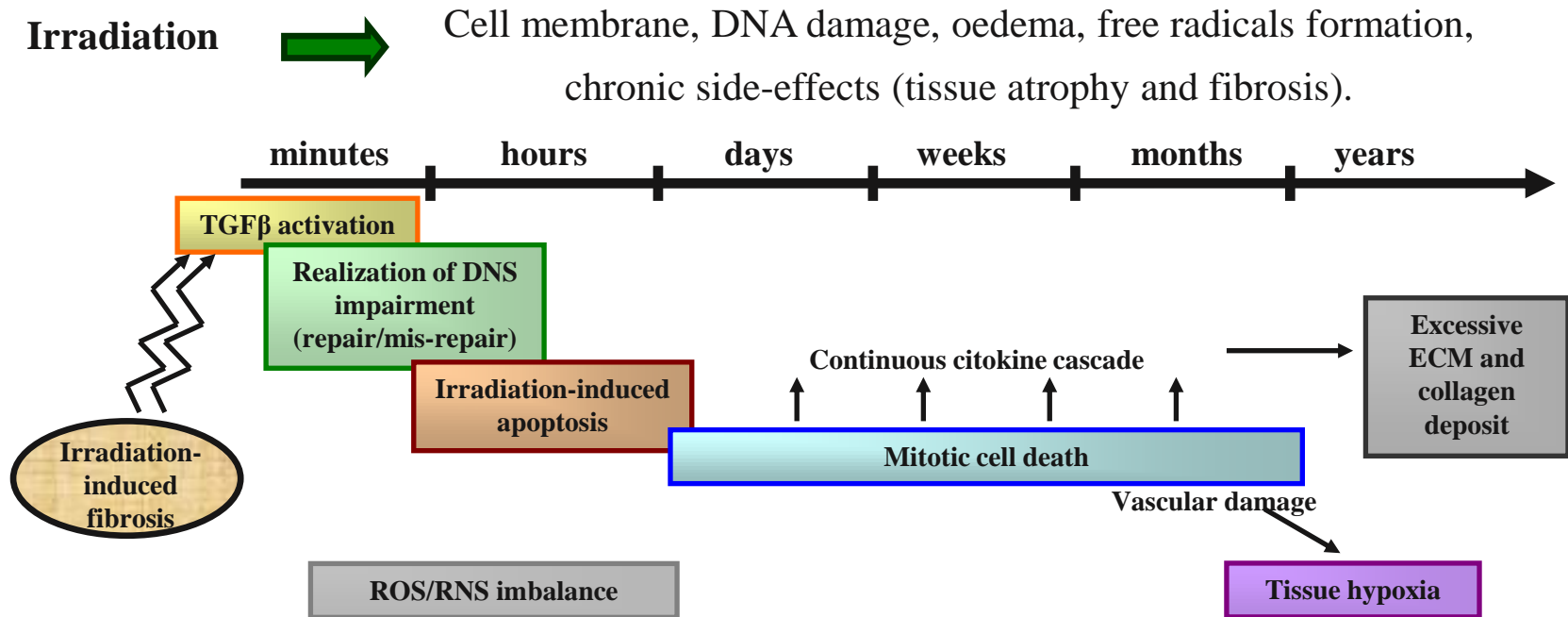


**HUNGARIAN
GOVERNMENT**

European Union
European Regional
Development Fund



INVESTING IN YOUR FUTURE



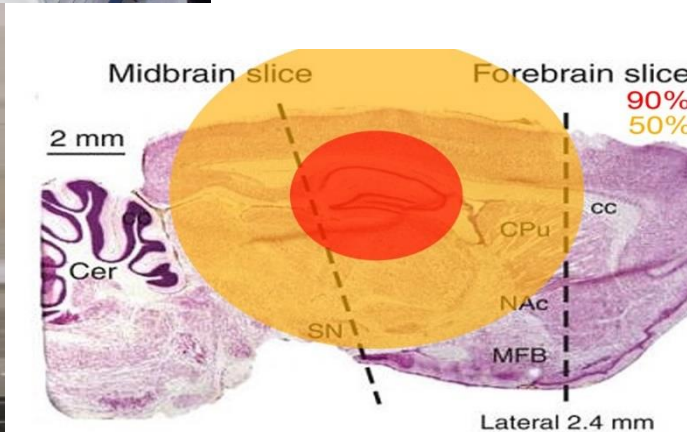
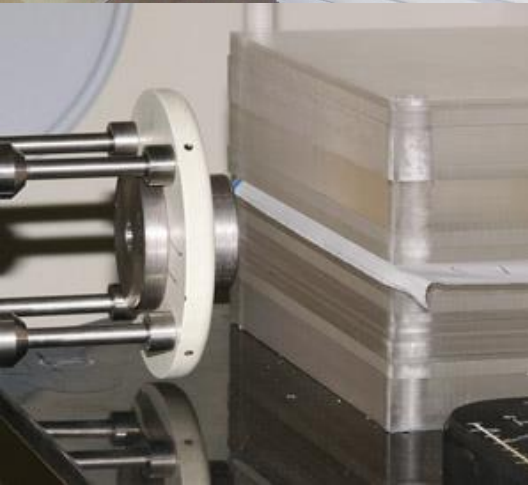
Acute project: Our aim was to examine the therapeutic effects of GPC after hippocampus irradiation-induced **acute peripheral inflammatory reactions**,

Chronic project: and to characterize the **chronic histological and functional consequences** of partial rat brain irradiation and to determine the effects of GPC.



Special collimators:

- Dose depth curve
- Field profile
- MU



A treatment planning study to assess the feasibility of laser-driven proton therapy using a compact gantry design

Treatment planning for radiotherapy with very high-energy electron beams and comparison of **VHEE** and VMAT plans

Medical physics aspects of the synchrotron radiation therapies: Microbeam radiation therapy (MRT) and synchrotron stereotactic radiotherapy (SSRT)

Image-guided microbeam irradiation to brain tumour bearing mice using a carbon nanotube X-ray source array

Energy Modulated Photon Radiotherapy: A Monte Carlo Feasibility Study

Energy- and intensity-modulated electron beams for radiotherapy

LET-painting increases tumour control probability in hypoxic tumours

New challenges in high-energy particle radiobiology

Simultaneous production of mixed electron--photon beam in a medical LINAC: A feasibility study.

Radiobiology network



TeWaTi
IR Fs laser
filamentation

**Proton/ion
MedAustron**
Laser driven proton
HZDR
OncoRay

DERMATOLOGY
Cellculture and
genetic lab

BRC
Xcelligence,
Tumor xenograft
DNA repair..

PATHOLOGY
Histology,
immunohistochem

ONCOTHERAPY
Dosimetry
RT planning, **linac**
foton, electron radiation

NEUROLOGY
RTPCR

Univ.Gödöllő
Fish
laboratory

**KFKI/BME/
ATOMKI**

RADIOLOGY
small animal
MRI

PHYSIOLOGY
neurovascular
function

**EXPERIMENTAL
SURGERY**
Oroboros,
protein level..

**APPLIED AND
ENVIRONMENTAL
CHEMISTRY**
Polymer gel
preparation

What is beyond the laser driven particle generation, acceleration?

Why is it worth to work on LD secondary sources for medicine?

Where we stand actually in laser based particle acceleration?

Where to go?

What is needed?

Why do we need laser driven ionizing radiation sources?

To enlarge the availability of charged particle beams: cost effective hadrontherapy
economic aspect

Provide special particle beams epithermic neutron, VHEE, microbeams, combined particle beams
physical aspect

To use the potential biological advantages of pulsed mode operation and ultra high dose rate- ultra high spatial and temporal resolution differential tumor- normal cell effect

biological aspect

Biomedical Application group at ELI-ALPS



Head of the Scientific Application
Division Péter Dombi (physicist)

Group leader: Katalin Hideghéty
(radiation oncologist)



and the group:

Róbert Polanek (medical physicist, physical background)

Emilia Rita Szabó (biologist, zebrafish experiments)

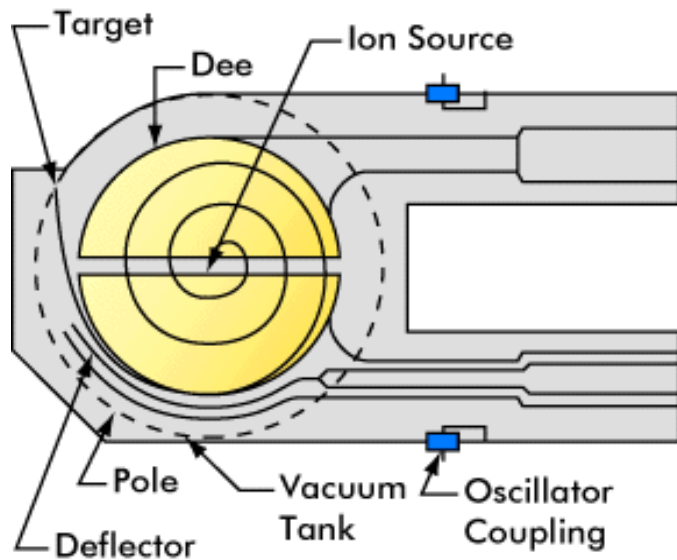
Bettina Ughy (chemist, cell culture experiments)

Zoltán Szabó (biologist, molecular examinations)

Tünde Tőkés (biologist, rodent experiments)

Cyclotron development

- | | |
|------|---|
| 1929 | Lawrence, inspired by Wideröe and Ising, conceives the cyclotron. |
| 1931 | Livingston demonstrates the cyclotron by accelerating hydrogen ions to 80 keV. |
| 1932 | Lawrence's cyclotron produces 1.25 MeV protons and he also splits the atom just a few weeks after Cockcroft and Walton (Lawrence received the Nobel Prize in 1939). |



Aims of our group/**ongoing projects**

Conventional X-ray beam

Femtosecond IR laser filamentation

Laser-electron beam

Laser-proton/ion beam

FACILITY DESIGN, RADIATION PROTECTION TRANSPORT AND POSITIONING OF THE BIOLOGICAL OBJECTS, **DOSIMETRY, DOSE CALCULATION,**



Development of *In vitro* and *in vivo* biological systems



Use of traditional *In vitro* and *in vivo* biological systems



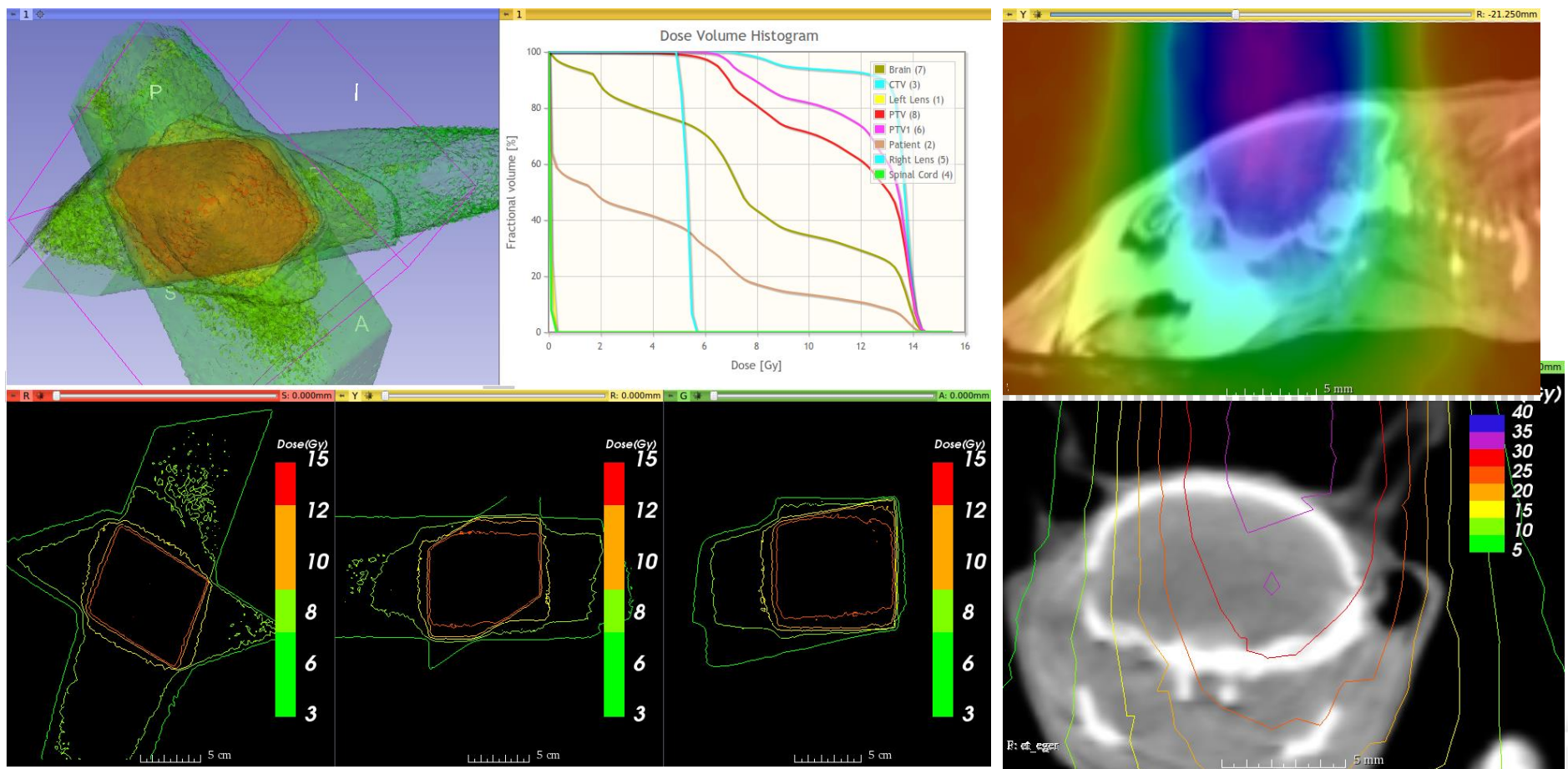
Use of validated *In vitro* and *in vivo* biological systems



Use of validated *In vitro* and *in vivo* biological systems

Evaluation of morphologic, functional, cellular, molecular changes, and comparison of these biological effects

Very High Energy Electron Beam VHEE



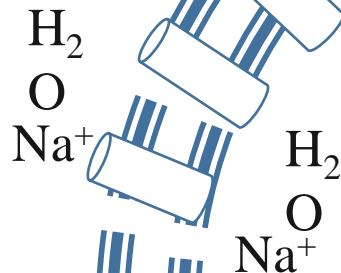
Subcellular effect of RT

Membrane damage

Massive Influx of Ca^{2+}

Swelling

Incr. perm.



Mitochondrial damage

SER

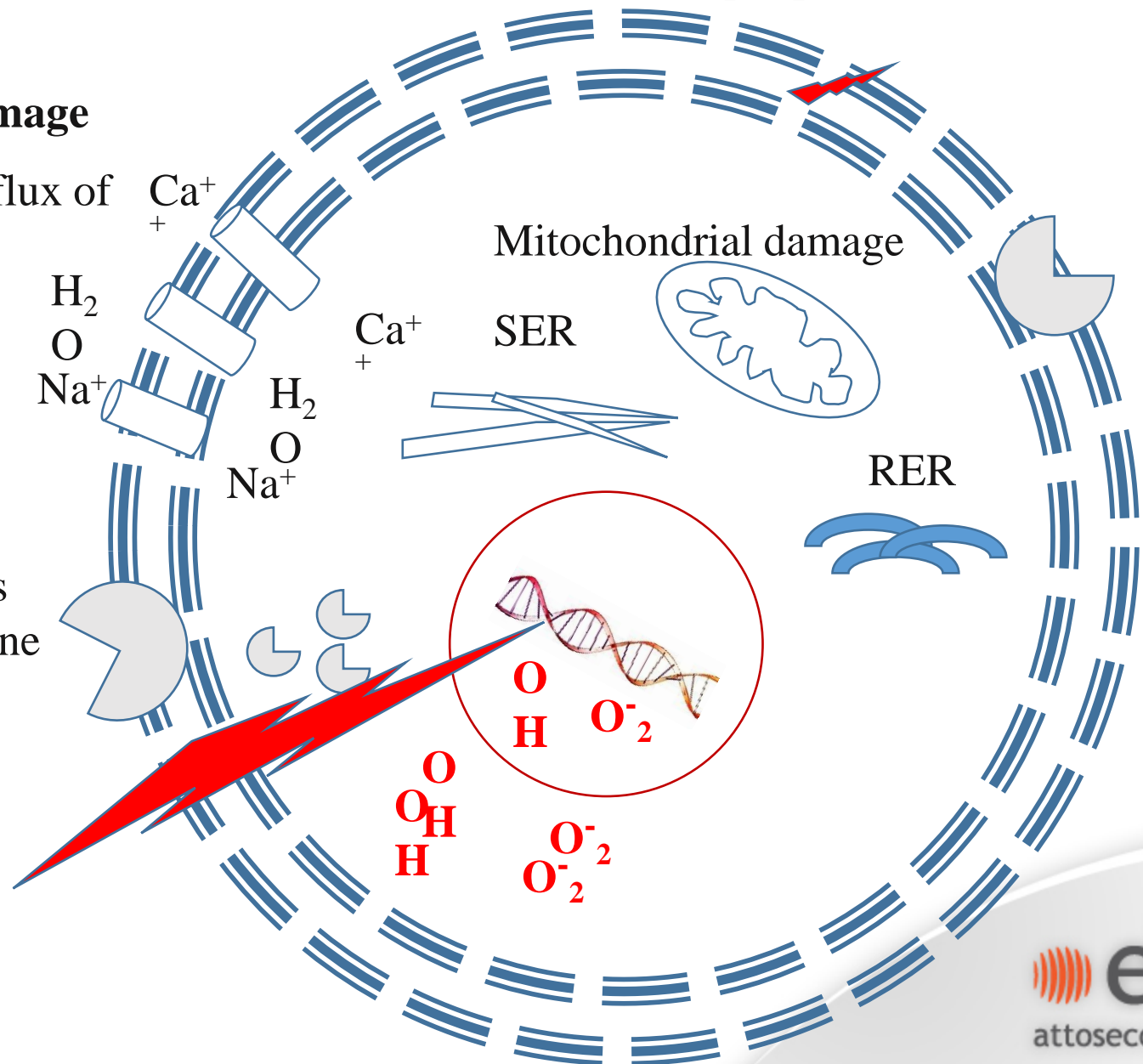
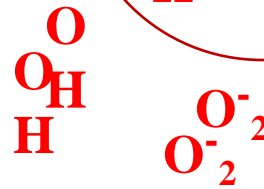
RER

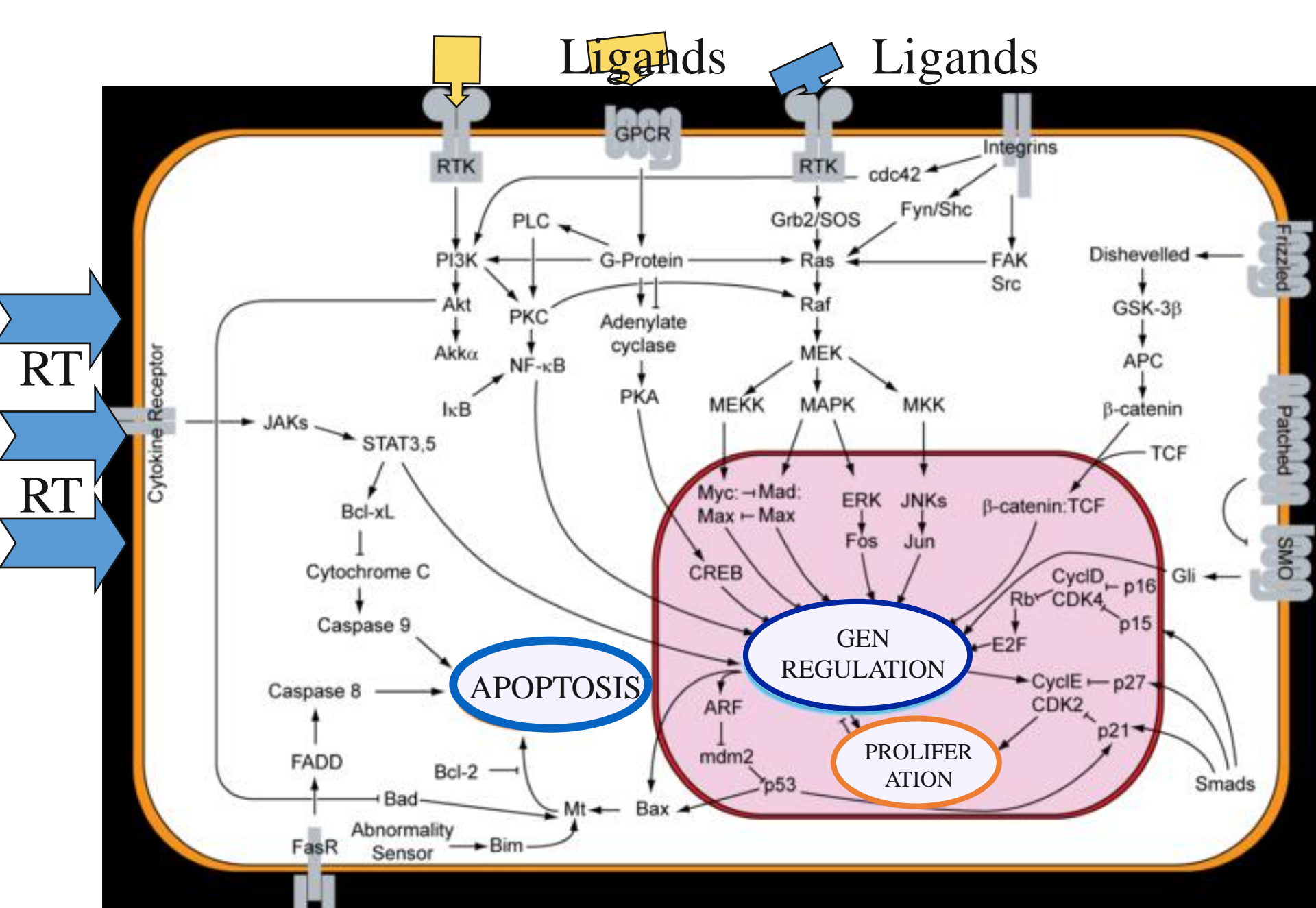
Lipid peroxidation

Protein damage

enzymes
membrane

DNA damage





RT

RT

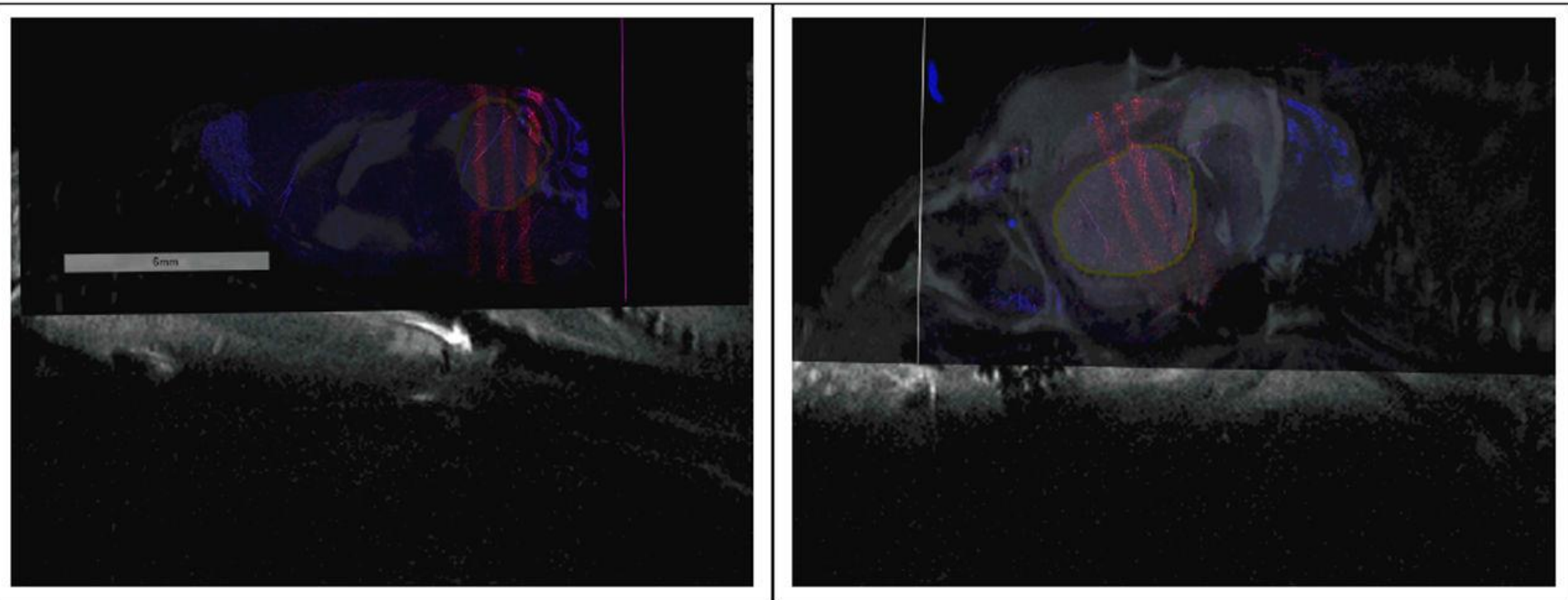
APOPTOSIS

GEN REGULATION

PROLIFERATION

Ongoing research on laser driven radiation

- Development of cost effective, compact, intensity and energy modulated, hospital based hadron therapy source
- Very high energy electron beam
- Radiation biology experiments to explore the potential biological advantages of
 - **pulsed mode operation**
 - **ultra high dose rate**
 - **ultra high spatial and temporal resolution**
potentially resulting in differential tumor - normal cell effects



γ -H2AX stained, sagittal image registered with MR projection for the same slice of tissue, from two animals irradiated with three microbeams of 48 Gy/beam

Our aims are to develop appropriate dosimetry system and preclinical models for Relative Biological Effectivity (RBE) investigation on laser driven particle beams.

- * **Frike liquid/gel chemical systems**
- * **Cancer and normal cell lines**
- * **Zebrafish embryos**
- * **Rodents (different organs/tumor)**

will be exposed to escalated doses of accelerator based photons, electrons, protons, carbon ions, photon-neutron mixed beam of a nuclear research reactor and laser driven very high energy electron-, and hadron beam.

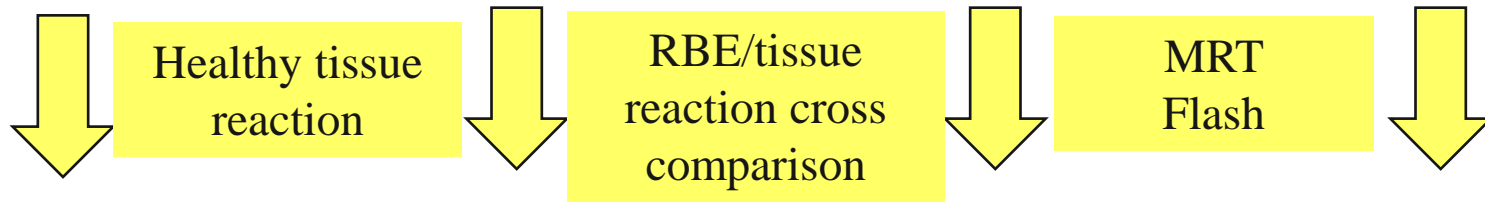
Conventional
RT sources

Laser-electron
beam

Laser-photon
beam

Laser-proton/ion
beam

SETUP DESIGN, DOSIMETRY, DOSE CALCULATION,



Classic *In vitro* and *in vivo* biological systems

Development of novel vertebrate model

Assessment of morphologic, functional, cellular, molecular changes
of different normal tissue and tumor models